Topological Order in 1-Dimensional Quantum Dipolar Gases
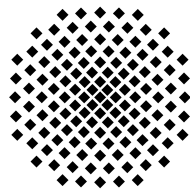
Universität Stuttgart

Germany

Yuan Miao

born in Shandong, China

Institut für Theoretische Physik III

Universität Stuttgart

A thesis submitted for the degree of

Master of Science

August 24, 2017

Supervisor: Prof. Dr. Hans Peter Büchler

Institut für Theoretische Physik III, Universität Stuttgart

Second Supervisor: Prof. Dr. Maria Daghofer

Institut für Funktionelle Materie und Quantentechnologien, Universität Stuttgart

Declaration

I herewith declare that I have produced this paper without the prohibited assistance of third parties and without making use of aids other than those specified; notions taken over directly or indirectly from other sources have been identified as such.

The thesis work was conducted from August 24, 2016 to August 24, 2017 under the supervision of Prof. Hans Peter Büchler at Institute for Theoretical Physics III, University of Stuttgart.

Stuttgart, August 24, 2017

Signature:

Abstract

Here we analyse the symmetry protected topological phases in 1 dimensional quantum gases with dipole-dipole interaction. Extended Bose Hubbard model and its spin-1 counterparts (AKLT model, Haldane chain model) are derived and their physical properties are explained. We focus on the symmetry protected nature of the Haldane phase in the models mentioned above, and obtain results concerning the edge modes and phase transitions. Moreover, it is obtained by analytic methods, e.g. bosonisation, that the long-range dipole-dipole interaction will not jeopardise the Haldane phase, and the phase transitions remain the same, too. Further development and connections to the state-of-the-art ultracold atom experiments are mentioned.

To my family

Contents

CONTENTS

Chapter 1

Introduction

La physique c'est comme un avion.
Quand ça s'arrête, ça tombe.

M. Peter

The physics of ultracold quantum gases has developed rapidly, from the technologies of laser cooling and the realisation of Bose Einstein condensate to ultracold atoms in optical lattices, opening a whole new chapter for the study of many-body physics both theoretically and experimentally [1, 2]. Due to the possible setups for low-dimensional systems, fine control of the interaction strength and the lack of disorders, ultracold atoms in optical lattices have become the ideal means to study the strongly correlated systems in 1 or 2 dimensions, e.g. Heisenberg model, Bose/Fermi Hubbard models, etc, comparing to some solid-state systems. Moreover, with state-of-the-art developments such as in situ microscopy and quasiparticle interference, it is also more convenient for ultracold atom experiments to study full-counting statistics and quasiparticle braiding statistics, which are more difficult to probe in the traditional solid-state experiments.

1.1 Dipolar atoms in optical lattices

Among all the current experimental methods, dipolar atoms in optical lattices enable long-range interactions, which attribute to quantum many-body phases, e.g. supersolid phases in extended Bose Hubbard model in 2 dimensions [3]. The characteristic features of dipole-dipole interaction is a polynomially decaying interaction that can be attractive or repulsive when two dipoles are head-to-tail or parallel, respectively [4].

More specifically, the dipole-dipole interaction can be written as

$$V_{dd}(\mathbf{r}) = \frac{(\mathbf{d})^2(1 - 3\cos^2\theta)}{\mathbf{r}^3}\frac{3\cos^2\phi - 1}{2},\tag{1.1}$$

where $\mathbf{d}$ is the electric dipole moment of dipolar atoms (for magnetic dipolar atoms, this term should be replaced by magnetic dipole moment μ), $\mathbf{r}$ is the distance between two dipolar atoms (usually the lattice spacing in optical lattices), θ is the angle between the (electric/magnetic) dipole precess axis and the distance between atoms, and ϕ is the tilt angle between dipole orientation and the precess axis.

There have been several researches on extended Bose Hubbard model (EBHM) in 1 dimension (1D) [5, 6], with a prediction of a Haldane insulating phase existing (explained explicitly in later chapter). Most of the previous work only takes into account the nearest-neighbour (NN) interaction, but the real physical systems with dipolar interaction has a polynomially decaying long-range interaction, which in principle could jeopardise the predicted Haldane insulating phase.

1.2   New paradigm of classification of matters

As we have mentioned, ultracold atoms in optical lattices provide opportunities to study strongly correlated systems, some of whose phases are described by Landau's paradigm of symmetry breaking, e.g. superconducting phase can be understood via global U(1) symmetry breaking, etc. It turns out that Landau's symmetry-breaking theory cannot describe all possible orders, for instance, the existence of different spin liquids with exactly the same symmetries. The solution to this problem is the discovery of topological orders, i.e. orders that are beyond the existence of local order parameters and long-range correlations.

There are several defining properties for matters with topological orders, e.g. no local order parameters, possibility of non-local order parameters, possibility of defining a topological invariant (i.e. invariant not depending on the local geometry of systems), and robustness against some local perturbation. Depending on whether the physical system is long-range or short-range entangled, the system has generic topological order or symmetry-protected topological (SPT) order. For instance, fractional quantum Hall systems and quantum spin liquids have generic topological orders, while topological insulators and topological superconductors only have SPT orders, i.e. robustness against

local perturbation that respects symmetries that protect the SPT orders. It has been proved that for 1D bosonic/spin systems, there cannot exist generic topological orders, leaving the possibilities of the existence of SPT or conventional symmetry breaking phases [7, 8, 9]. In fact, SPT phases have brought many new insights into condensed matter physics. Most notably, the non-dissipative edge states of topological insulators have been proposed for spintronics applications, and defects in topological superconductors could be used for topological quantum computation due to the non-Abelian nature.

More importantly, for 1D p-wave superconductor, edge modes (i.e. Majorana zero-modes) have been discovered with non-Abelian braiding statistics in quasi-1D network [10, 11, 12, 13]. For some bosonic SPT, edge modes are expected, but many physical properties of edge modes are not clear. We study the properties of edge modes in Affleck-Kennedy-Lieb-Tasaki (AKLT) model (i.e. a model with ground states of SPT phase), and summarise the properties of edge modes with notable examples that have been studied in this thesis.

In this thesis, we show that the Haldane phase exists in EBHM in 1D and its spin counterparts, i.e. Haldane chain and AKLT model. Edge modes of AKLT model are studied, with a summary of previous work on similar topic. Moreover, we study the impact of long-range interaction, e.g. dipole-dipole interaction, to the existing Haldane phase using bosonisation, and obtain the conclusion that dipole-dipole interaction in 1D will not jeopardise the Haldane phase, matching with the prediction from previous work using numerical methods.

1.3   Outline of the thesis

The main purpose of this thesis is to present a field-theoretical method to analyse the effect of long-range interaction on SPT phases in EBHM as well as edge modes in some models exhibiting SPT phases. Some methods and examples used in this thesis are introduced pedagogically. In Chapter 2, we summarise the theoretical models that have been studied in the later chapters with the derivation from more physically realistic setups. Then in Chapter 3, we present the analytic and numerical methods that are used extensively in this thesis. Chapter 4 gives a detailed analysis on AKLT model, from which we define edge mode operators and study their properties. A fixed-point

model of AKLT model is also proposed via real space renormalisation method. Chapter 5 is devoted to the results for the study of the effect of long-range interaction (e.g. dipole-dipole interaction) on SPT phases, which identifies the phases that have been predicted in several previous papers, proving that with the presence of dipole-dipole (or even longer-range) interaction, the SPT phases and the according phase transitions remain. We also note that with the breakdown of bosonisation calculation due to longer-range interaction. We then compare the results obtained for spin-1 models with EBHM in Chapter 6, with similar SPT phase and the absence of edge mode. Moreover, it is possible to examine our theory of Haldane phase in the presence of long-range interaction with state-of-the-art ultracold atom experiment. Eventually we summarise our work and give some insights for further research in Chapter 7.

Chapter 2

Theoretical Models

<div align="right">

If it disagrees with experiment, it is wrong.

Richard Feynman
</div>

In this chapter we derive the mainly used theoretical models in this thesis from a realistic setup of dipolar atoms in optical lattices. (Extended) Bose Hubbard model can be derived directly from bosonic atoms in optical lattices [4, 14, 15], with the presence of a s-wave scattering (and dipole-dipole interaction). Meanwhile, when on-site repulsion U is large, one can truncate the bosonic Hilbert space to finite dimensions, giving the possibility to map the bosonic model into a spin counterpart. In our case, we map the 1D EBHM into a spin-1 Haldane chain model, which could have the same SPT phase as another spin-1 toy model, Affleck-Lieb-Kennedy-Tasaki (AKLT) model. Those three models mentioned are the main objects investigated in the later chapters.

2.1 Extended Bose Hubbard model from dipolar atoms in optical lattices

We are interested in the behaviour of bosons trapped in a periodic optical potential (V_opt) as well as a magnetic harmonic trap (V_ho), which the potential from the external fields is given as

$$
\begin{aligned}
U_\text{ext}(\mathbf{r}) &= U_\text{opt}(\mathbf{r}) + U_\text{ho}(\mathbf{r}) \\
&= \sum_{i=x,y,z} U_{0,i} \cos^2(k_i r_i) + \frac{1}{2} \sum_{i=x,y,z} \omega_i^2 r_i^2,
\end{aligned}
\tag{2.1}
$$

where $(U_{0,x}, U_{0,y}, U_{0,z})$ is the depth of the optical lattice in spatial directions, and $(\omega_x, \omega_y, \omega_z)$ are the frequencies of the harmonic potential [14].

If the temperature of the atomic gas is very low, i.e. $T \to 0$, together with a low density of the atomic gas, only s-wave scattering could take place, which can be effectively understood as a contact interaction, solely determined by the s-wave scattering length a_s,

$$U_{\text{eff}}(\mathbf{r}) = g\delta^{(3)}(\mathbf{r}), \ g = \frac{4\pi\hbar^2 a_s}{m}. \tag{2.2}$$

Taking into account the kinetic energy of the atoms and chemical potential μ, we can write down the Hamiltonian of bosonic atoms in optical lattices with contact interaction in terms of second quantisation (i.e. $\psi^\dagger(\mathbf{r})$ and $\psi(\mathbf{r})$ are bosonic creation and annihilation operators) as

$$H = \int d^3 r \psi^\dagger(\mathbf{r}) \left[-\frac{\hbar^2 \nabla^2}{2m} + U_{\text{ext}}(\mathbf{r}) + \frac{g}{2}\psi^\dagger(\mathbf{r})\psi(\mathbf{r}) - \mu \right] \psi(\mathbf{r}), \tag{2.3}$$

where $U_{\text{ext}}(\mathbf{r}) = U_{\text{opt}}(\mathbf{r}) + U_{\text{ho}}(\mathbf{r})$ is the external potential in Eq. 2.1, and the contact potential in Eq. 2.2 is included. The chemical potential μ fixes the total number of bosonic atoms, i.e. the system can be considered as a grand canonical ensemble.

The bosonic field operators can be written in terms of single-particle wavefunctions $\{\Phi_n(\mathbf{r})\}$ with n as a complete set of single-particle quantum numbers,

$$\psi(\mathbf{r}) = \sum_n \Phi_n(\mathbf{r})a_n, \ \psi^\dagger(\mathbf{r}) = \sum_n \Phi_n^*(\mathbf{r})a_n^\dagger, \tag{2.4}$$

where $a_n^\dagger$ and a_n are creation and annihilation operators of mode n with commutation relation $[a_n, a_n^\dagger] = 1$. Hence, the field operators obey commutation relations of bosons

$$[\psi(\mathbf{r}), \psi^\dagger(\mathbf{r}')] = \sum_{n=0}^{\infty} \Phi_n(\mathbf{r})\Phi_n^*(\mathbf{r}') = \delta^{(3)}(\mathbf{r} - \mathbf{r}'), \tag{2.5}$$

$$[\psi(\mathbf{r}), \psi(\mathbf{r}')] = [\psi^\dagger(\mathbf{r}), \psi^\dagger(\mathbf{r}')] = 0. \tag{2.6}$$

We can approximate the bosonic field operators with Wannier functions $w_q(\mathbf{r} - \mathbf{R}_i)$ with band indices q and they are localised and centered around the lattice site R_i [4], since the alternating optical lattices are deep, which implies the applicability of tight binding approximation

$$\psi(\mathbf{r}) = \sum_{a,i} w_q(\mathbf{r} - \mathbf{R}_i)a_{q,i}, \tag{2.7}$$

$$\psi^\dagger(\mathbf{r}) = \sum_{a,i} w_q^*(\mathbf{r} - \mathbf{R}_i)a_{q,i}^\dagger. \tag{2.8}$$

2.1 Extended Bose Hubbard model from dipolar atoms in optical lattices

If the temperature is low enough not to induce interband transition, we can restrict our theory only to the lowest Bloch band, which simplifies our theory. Therefore, we can rewrite the continuous theory into a lattice one. The Hamiltonian 2.3 becomes [4]

$$H = -\sum_{i,j} t_{i,j} a_i^\dagger a_j + \sum_{i,j,k,l} \frac{U_{ijkl}}{2} a_i^\dagger a_j^\dagger a_k a_l - \sum_{i,j} \mu_{i,j} a_i^\dagger a_j, \qquad (2.9)$$

where the quantities in Eq. 2.9 are

$$t_{ij} = -\int d^3 r\, w^*(\mathbf{r} - \mathbf{R}_i) \left[-\frac{\hbar^2 \nabla^2}{2m} + U_{\mathrm{opt}}(\mathbf{r}) w(\mathbf{r} - \mathbf{R}_j) \right], \qquad (2.10)$$

$$U_{ijkl} = g \int d^3 r\, w^*(\mathbf{r} - \mathbf{R}_i) w^*(\mathbf{r} - \mathbf{R}_j) w(\mathbf{r} - \mathbf{R}_k) w(\mathbf{r} - \mathbf{R}_l), \qquad (2.11)$$

$$\mu_{ij} = \int d^3 r\, w^*(\mathbf{r} - \mathbf{R}_i)[\mu - U_{\mathrm{ho}}(\mathbf{r})] w(\mathbf{r} - \mathbf{R}_j). \qquad (2.12)$$
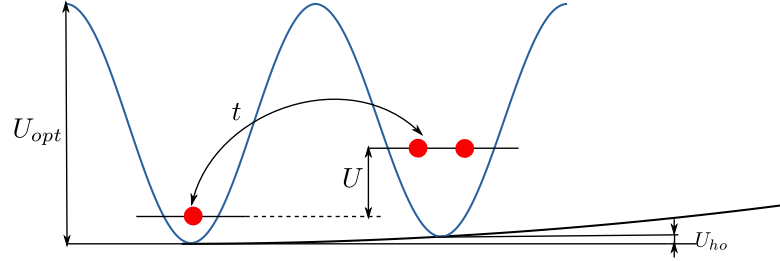
Figure 2.1: A schematic sketch of Bose Hubbard model [4, 14].

Due to the deep optical lattices, the Wannier functions are localised near the centre of lattice sites. So we could get the dominant contributions in 2.11 and 2.12 are U_{iiii} and μ_{ii}. For the kinetic energy part, if we assume that the Wannier functions have Gaußian form, the main contribution will be t_{ij} (with a constant contribution of t_{ii}) with site j as the nearest-neighbour site of site i. Therefore, we derive the Bose Hubbard model Hamiltonian [14, 15]

$$H_{\mathrm{BH}} = -t \sum_{\langle ij \rangle} a_i^\dagger a_j + \frac{U}{2} \sum_i n_i(n_i - 1) - \sum_i \mu_i n_i, \qquad (2.13)$$

where $\langle ij \rangle$ denotes the nearest-neighbour relation of sites i and j, number operator $n_i = a_i^\dagger a_i$, on-site interaction $U = g \int d^3r \mid w(\mathbf{r}) \mid^2$, and tunnelling coefficient $t = t_{ij} = t_{ji}$. In this thesis, we mainly discuss about 1D system, hence, the 1D Bose Hubbard model can be written as

$$H_{\text{BH}} = -t \sum_i (a_i^\dagger a_{i+1} + \text{h.c.}) + \frac{U}{2} \sum_i n_i(n_i - 1) - \sum_i \mu_i n_i. \qquad (2.14)$$

After we consider the effect of the dipole-dipole interaction (cf. Eq. 1.1), we can rewrite the second-quantised Hamiltonian 2.3 as

$$\begin{aligned} H = \int d^3r \psi^\dagger(\mathbf{r}) \left[-\frac{\hbar^2 \nabla^2}{2m} + U_{\text{ext}}(\mathbf{r}) + \frac{g}{2} \psi^\dagger(\mathbf{r}) \psi(\mathbf{r}) - \mu \right] \psi(\mathbf{r}) \\ + \frac{1}{2} \int d^3r_1 d^3r_2 \psi^\dagger(\mathbf{r}_1) \psi^\dagger(\mathbf{r}_2) V_{\text{dd}}(\mathbf{r}_1 - \mathbf{r}_2) \psi(\mathbf{r}_1) \psi(\mathbf{r}_2), \end{aligned} \qquad (2.15)$$

where $V_{\text{dd}} = \frac{\mu_0 \mu^2}{4\pi} \frac{1}{\mathbf{r}^3}$ is the dipole-dipole interaction between dipolar atoms.

We use the similar method as getting the Bose Hubbard Hamiltonian with lattice sites, i.e. expanding the bosonic field operators in terms of Wannier functions. Thus the dipole-dipole term becomes

$$H_{\text{dd}} = \sum_{i,j,k,l} \frac{V_{i,j,k,l}}{2} a_i^\dagger a_j^\dagger a_k a_l, \qquad (2.16)$$

with the matrix elements $V_{i,j,k,l}$ as

$$V_{i,j,k,l} = \int d^3r_1 d^3r_2 w^*(\mathbf{r}_1 - \mathbf{R}_i) w^*(\mathbf{r}_2 - \mathbf{R}_j) V_{\text{dd}}(\mathbf{r}_1 - \mathbf{r}_2) w(\mathbf{r}_1 - \mathbf{R}_k) w(\mathbf{r}_2 - \mathbf{R}_l). \quad (2.17)$$

As we have already explained, the Wannier functions are strongly localised around the lattice sites, which simplify the expression in Eq. 2.17 with only two contributions left, i.e. on-site ($i = j = k = l$) and off-site ($i = k \neq j = l$) terms.

The on-site terms have similar expressions as the contact interaction terms, so we can combine these two kinds of terms and renormalise the parameter U in the Hamiltonian.

For the off-site terms, the matrix elements reduce to

$$V_{ijij} \simeq V_{\text{dd}}(\mathbf{R}_1 - \mathbf{R}_2) \int d^3r_1 \mid w(\mathbf{r}_1 - \mathbf{R}_1) \mid^2 \int d^3r_2 \mid w(\mathbf{r}_2 - \mathbf{R}_2) \mid^2, \qquad (2.18)$$

for the sake of simplicity, we denote V_{ijij} as $\frac{1}{r^3} V_{i,i+r}$, where $j = i + r$ and we specify the spatial dependence (in 1D) of the dipole-dipole interaction.

Thus, the off-site terms can be expressed as

$$H_{\mathrm{dd}}^{\mathrm{off-site}} = \sum_{i,r>0} \frac{V_{i,i+r}}{r^3} n_i n_{i+r}. \tag{2.19}$$

Eventually we get a Hamiltonian known as extended Bose Hubbard model (EBHM) [4, 5], i.e.

$$H_{\mathrm{EBHM}} = -t \sum_{\langle ij \rangle} a_i^\dagger a_j + \frac{U}{2} \sum_i n_i(n_i - 1) - \sum_i \mu_i n_i + \sum_{i,r>0} \frac{V_{i,i+r}}{r^3} n_i n_{i+r}. \tag{2.20}$$

In this thesis, we study the 1D EBHM with only nearest-neighbour interaction (which is a good approximation to start with), and later we add the entire long-range interaction terms. The Hamiltonian of 1D EBHM with nearest-neighbour interaction becomes

$$H_{\mathrm{EBHM}} = -t \sum_i (a_i^\dagger a_{i+1} + \mathrm{h.c.}) + \frac{U}{2} \sum_i n_i(n_i - 1) - \sum_i \mu_i n_i + V \sum_i n_i n_{i+1}. \tag{2.21}$$

From now on, without specification, 1D EBHM refers to 1D EBHM with only nearest-neighbour interaction.

2.2 Spin-1 models from extended Bose Hubbard model

Bosonic models sometimes can be mapped into spin counterparts, with more analytic methods available to understand their physical properties. There is one big distinction between bosonic and spin models, i.e. the bosonic Hilbert space of a local site has infinity dimensions while the spin local Hilbert space only have finite dimensions. In 1D EBHM (i.e. Eq. 2.21), when the on-site repulsion U is large, it is reasonable to restrict the possible occupation state number of bosons per site to 3 (i.e. 0, 1, or 2 bosons per site are allowed), which truncates the local Hilbert space into a 3-dimensional one. This gives us the hint that we can map 1D EBHM into a spin-1 chain, which could faithfully describe the same phases [5, 6, 16].

We use Holstein-Primakoff mapping that maps spin operators into bosonic ones (and vice versa)

$$\begin{aligned}
S_i^+ &= a_i^\dagger \sqrt{2\bar{n} - a_i^\dagger a_i}, \\
S_i^- &= \sqrt{2\bar{n} - a_i^\dagger a_i}\, a_i, \\
S_i^z &= a_i^\dagger a_i - \bar{n},
\end{aligned} \tag{2.22}$$

where $a_i^\dagger$, a_i are bosonic creation and annihilation operators, $\bar{n}$ is the average number of bosons per site. One can easily check that the mapped bosonic/spin operators satisfy the commutation relations between operators.

As we can see, the Holstein-Primakoff mapping is local and unitary. In addition, it maps models of bosons with average filling of $\bar{n}$ to a spin-$\bar{n}$ models, with a constraint of $a_i^\dagger a_i < 2\bar{n}$. This is satisfied in 1D EBHM with average filling $\bar{n} = 1$.

In the case of 1D EBHM with average filling $\bar{n} = 1$, one can get the mapped spin-1 model as

$$H_{\text{spin}} = -t \sum_i (S_i^+ S_{i+1}^- + \text{h.c.}) + \frac{U}{2} \sum_i (S_i^z)^2 + V \sum_i S_i^z S_{i+1}^z + \Delta H, \qquad (2.23)$$

$$
\begin{aligned}
\Delta H = -t\xi \sum_i [&S_i^z S_{i+1}^+ S_{i+1}^- + S_i^- S_i^z S_{i+1}^+ + S_i^- S_{i+1}^+ S_{i+1}^+ + \\
&S_i^+ S_{i+1}^- S_{i+1}^z + \xi(S_i^z S_i^+ S_{i+1}^- S_{i+1}^z + S_i^+ S_i^z S_{i+1}^z S_{i+1}^-)],
\end{aligned}
\qquad (2.24)
$$

assuming that the chemical potential is homogeneous (leading to a constant in Hamiltonian that have been omitted here), and $\xi = \sqrt{(\bar{n}+1)/\bar{n}} - 1 = \sqrt{2} - 1$. ΔH term comes from the fact that $\sqrt{2 - n_i}$ terms in the Holstein-Primakoff mapping 2.22 is highly non-linear. This term will become important when we consider the symmetries protecting the SPT phase, but for now we omit it for simplicity. And as a consequence, we obtain the Haldane chain Hamiltonian

$$H_{\text{spin}} = t \sum_i (S_i^+ S_{i+1}^- + \text{h.c.}) + \frac{U}{2} \sum_i (S_i^z)^2 + V \sum_i S_i^z S_{i+1}^z. \qquad (2.25)$$

Here we have performed a staggered transformation of adjacent spins, i.e. $S_i^{x/y} \rightarrow (-1)^i S_i^{x/y}$, which changes the sign of t term, and since the transformation is canonical, the physics remains the same. The spin model that we obtained is the renowned Haldane chain model, consisting of 1D spin-1 XXZ model and on-site $(S^z)^2$ term. Haldane chain model has been previously studied via non-linear σ model [17], and numerical methods [5, 7], revealing the existence of a symmetry-protected topological phase. We will analyse Haldane chain model in details in later chapters.

Despite the long history of studying Haldane chain model, it is difficult to obtain the exact ground states in the SPT phase, which are believed to have fourfold degeneracy. After the seminal paper by Haldane that predicted a gapped phase later identified as

a symmetry-protected phase, Affleck, Kennedy, Lieb and Tasaki discovered another spin-1 model with the same SPT order, i.e. AKLT model [18, 19].

$$H_{\text{AKLT}} = \sum_i \mathbf{S}_i \cdot \mathbf{S}_{i+1} + \frac{1}{3}(\mathbf{S}_i \cdot \mathbf{S}_{i+1})^2. \tag{2.26}$$

The advantage of studying AKLT model (Eq. 2.26) is that the ground states can be constructed exactly, from which one can easily calculate the correlation functions and identify the edge mode operators within the ground state manifold. AKLT model will be discussed in details in the following chapters.

Chapter 3

Methods

In this chapter we introduce methods that are used to analyse EBHM, Haldane, and AKLT models in a concise manner. We use both analytic and numerical methods in this thesis, namely bosonisation, density matrix renormalisation group (DMRG), and using matrix product states (MPS) to classify bosonic/spin SPT phases.

3.1   Bosonisation

Bosonisation is an analytic field theory that describes the effective low-energy sectors of 1D interacting fermionic (or spin-1/2 via Jordan-Wigner transformation) models as free bosonic field theories in continuous limit [20, 21, 22]. It follows by an observation that 1D fermionic particle-hole excitations can be rewritten in terms of a bosonic field creation/annihilation operators.

3.1.1   Bosonisation for 1D free spinless fermions

We start from a free fermion Hamiltonian

$$H = \sum_n c_n^\dagger c_{n+1} + \text{h.c.}, \tag{3.1}$$

from which we could obtain a dispersion relation $E \propto \cos(kx)$. From the cosine dispersion relation of free fermions, we can deduce that it is reasonable to treat dispersion

relation in the vicinity of $k = \pm k_F$ linearly [20, 22], namely

$$c_n^\dagger \sim \psi_R^\dagger(x_n)e^{-ik_F x_n} + \psi_L^\dagger(x_n)e^{ik_F x_n}, \qquad (3.2)$$

$$c_n \sim \psi_R(x_n)e^{ik_F x_n} + \psi_L(x_n)e^{-ik_F x_n}, \qquad (3.3)$$

where $c_n^\dagger$ and c_n are fermionic creation and annihilation operators respectively. $\psi_R(x_n)$ and $\psi_L(x_n)$ in continuous limit correspond to the right-moving and left-moving fermions, containing only long wavelength components.
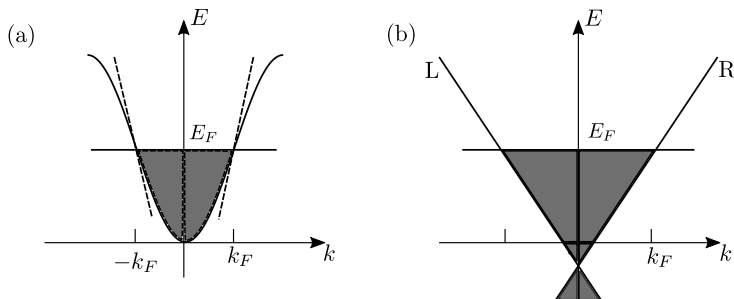
Figure 3.1: Dispersion relation of free fermions (a) is replaced by a linear dispersion relation (b). It is natural to obtain the right/left moving fermions from such a linear dispersion [20].

Density fluctuation of fermionic field can be written in terms of particle-hole excitations, i.e.

$$\rho^\dagger(q) = \sum_k c_{k+q}^\dagger c_k. \qquad (3.4)$$

An naïve observation would be that if the density fluctuation of momentum is a bona fide excitation, it can be described by bosonic operators b_q and $b_q^\dagger$. The virtue of rewriting the density fluctuations as bosonic operators would be the interaction Hamiltonian term $H_{int} \propto \rho(q)\rho(-q)$ is quadratic with regard to bosonic operators [20], and thus can be considered as a free boson theory.

To be more precise, we need to use normal ordered operators to denote density fluctuation operators $\rho(q)$, because we use a linear dispersion relation near Fermi points, resulting in an infinite occupation numbers of fermions [20]. Hence, a normal ordered operator is

$$:AB := AB - \langle 0 | AB | 0 \rangle, \qquad (3.5)$$

where $|0\rangle$ is the ground state, e.g. in fermionic case, the Fermi sea.

The normal ordered density operator is defined as

$$:\rho_r(x):=:\psi_r^\dagger(x)\psi_r(x):, \tag{3.6}$$

where r can be either R or L, representing right and left mover, respectively. $\psi_r(x) = \sum_k e^{ikx} c_{r,k}$ is the continuous limit (i.e. fermionic field operator) of the fermionic annihilation operators in a lattice, and $\psi_r^\dagger(x)$ is defined accordingly.

After Fourier transformation, we obtain

$$\begin{aligned}:\rho_r^\dagger(p): &= \sum_k c_{r,k+p}^\dagger c_{r,k}, \ (p \neq 0)\\ &= \sum_k :c_{r,k}^\dagger c_{r,k}:= N_r, \ (p = 0)\end{aligned} \tag{3.7}$$

where N_r can be understood as the number of right or left particle-hole excitations [20, 21]. Since $\rho_r(x)$ is Hermitian, we can easily obtain $\rho_r^\dagger(p) = \rho_r(-p)$. Moreover, we can obtain the commutation relation

$$[\rho_r^\dagger(p), \rho_{r'}^\dagger(-p')] = -\delta_{r,r'}\delta_{p,p'}\frac{rpL}{2\pi}, \tag{3.8}$$

where r in the last expression is ± 1, corresponding to right or left mover, respectively, and L is the system size. Eq. 3.8 is remarkable, since it is bosonic commutation relation up to a renormalisation constant, confirming our conjecture of density fluctuation operators can be linked to bosonic operators.

Thus we can define the boson creation and annihilation operators as

$$\begin{aligned}b_p^\dagger &= \sqrt{\frac{2\pi}{L|p|}} \sum_r \Theta(rp)\rho_r^\dagger(p),\\ b_p &= \sqrt{\frac{2\pi}{L|p|}} \sum_r \Theta(rp)\rho_r^\dagger(-p),\end{aligned} \tag{3.9}$$

where $\Theta(p)$ is the Heaviside step function.

Since we have a bona fide bosonic field to describe the particle-hole excitations, it is natural to express the original fermionic fields with the new bosonic language. After some algebraic calculations,

$$[b_p, H] = v_F p b_p, \tag{3.10}$$

3. METHODS

$$[\rho_r^\dagger(p), \psi_r(x)] = -e^{ipx}\psi_r(x), \tag{3.11}$$

suggesting that $H \propto \sum_p b_p^\dagger b_p$, and $\psi_r(x) \propto \exp \sum_p e^{ipx}\rho_r(p)\frac{2\pi r}{pL}$. Taking into account the anti-commuting nature of fermion field operator $\psi_r(x)$, a more accurate expression is

$$\psi_r(x) = F_r \exp \sum_p e^{ipx}\rho_r(p)\frac{2\pi r}{pL}, \tag{3.12}$$

where F_r is called Klein factor, which has an anti-commuting relation among different Klein factors while commuting with bosonic operators. The physical meaning of Klein factor would be that $F_r^\dagger/F_r$ acting on a physical state will add/remove a fermion from the physical system, due to the fact that bosonic operators cannot change the total number of fermions in the system.

Thus it is convenient to define two bosonic fields $\phi(x)$ and $\theta(x)$ as

$$\begin{aligned}
\phi(x) &= -(N_R + N_L)\frac{\pi x}{L} - \frac{i\pi}{L}\sum_{p\neq 0}\frac{1}{p}e^{-\alpha|p|/2-ipx}[\rho_R^\dagger(p) + \rho_L^\dagger(p)], \\
\theta(x) &= (N_R - N_L)\frac{\pi x}{L} + \frac{i\pi}{L}\sum_{p\neq 0}\frac{1}{p}e^{-\alpha|p|/2-ipx}[\rho_R^\dagger(p) - \rho_L^\dagger(p)],
\end{aligned} \tag{3.13}$$

where $\alpha \to 0$ is introduced to avoid divergence when momentum $p \to \infty$, i.e. introducing a momentum cutoff $\Lambda \sim \frac{1}{\alpha}$.

Utilising the field operators in Eq. 3.13, we obtain the expression of free fermion Hamiltonian 3.1 and fermionic field operator 3.12

$$H = \sum_{p\neq 0} v_F|p|b_p^\dagger b_p + \frac{\pi v_F}{L}\sum_r N_r^2, \tag{3.14}$$

$$\psi_r(x) = F_r \lim_{\alpha\to 0}\frac{1}{\sqrt{2\pi\alpha}}e^{ir(k_F-\pi/L)x}e^{-i(r\phi(x)-\theta(x))}. \tag{3.15}$$

Using the commutation relations of bosons, we can attain the commutation relations between fields $\phi(x)$ and $\theta(x)$

$$[\phi(x), \theta(x')] = \sum_{p\neq 0}\frac{\pi}{Lp}e^{ip(x'-x)-\alpha|p|} = i\frac{\pi}{2}sgn(x'-x), \ \alpha \to 0, \tag{3.16}$$

$$[\phi(x), \frac{1}{\pi}\nabla\theta(x')] = i\delta(x'-x). \tag{3.17}$$

Eq. 3.17 shows that $\Pi(x) = \frac{1}{\pi}\nabla\theta(x)$ is the conjugate momentum of field $\phi(x)$ [20, 23]. When $L \to \infty$, i.e. thermodynamic limit, using Eq. 3.13,

$$\frac{1}{\pi}\nabla\phi(x) = -[\rho_R(x) + \rho_L(x)], \frac{1}{\pi}\nabla\theta(x) = \rho_R(x) - \rho_L(x). \tag{3.18}$$

Obviously, $\nabla\phi(x)$ is proportional to the density fluctuation at point x, while $\nabla\theta(x)$ is proportional to the current in 1D. Thus, Hamiltonian 3.14 is modified as (omitting constant terms)

$$H = \frac{v_F}{2\pi}[(\nabla\theta(x))^2 + (\nabla\phi(x))^2]. \tag{3.19}$$

This is the celebrated Luttinger liquid Hamiltonian [20, 21, 23, 24], and we have mapped a free spinless fermionic theory into a free bosonic one (in fact, the bosonic theory is for free compactified bosons, which is more obvious if one looks at the correlation functions of free fermions and compactified bosons. More detailed explanation is available in [20, 23, 25] and references therein).

3.1.2   Bosonisation with interactions

Previously we have considered the Hamiltonian for free spinless fermions. It turns out that free spinless fermion Hamiltonian can be mapped into a free (compactified) bosonic one. It is trivial to show that without interaction, free spinful fermion Hamiltonian can be mapped to a free bosonic one with two flavours as well (i.e. two decoupled sets of bosonic fields), but what will the bosonic Hamiltonian look like after including the interactions?

We can consider the interactions between fermions as a scattering process, see Fig. 3.2. More interestingly, g_1 term is the Umklapp process, which could bring a spin gap as shown later.
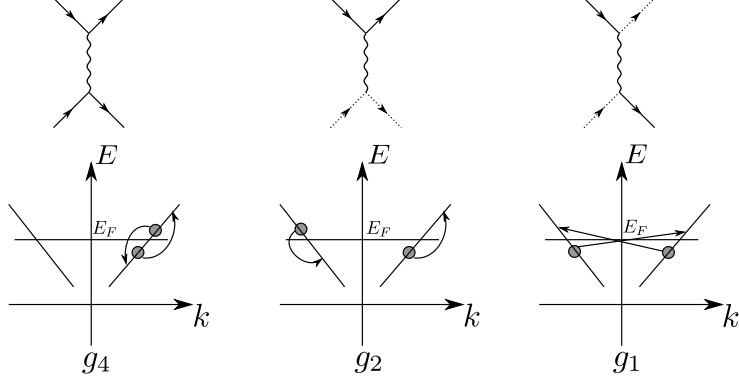
Figure 3.2: The low-energy scattering process. Dashed line refers to a left-moving fermion, while a full line refers to a right-moving fermion. The names g_1, g_2, g_4 come from so called g-ology [20]. In addition, if the spin of the two electrons are equal, the interaction takes value of $g_\parallel$, and $g_\perp$ for opposite spins.

For the interaction localised at $q \to 0$, i.e. g_2, g_4 terms, we can get

$$H_4 = \int dx \sum_{r=R,L} \sum_{s=\uparrow,\downarrow} \left[\frac{g_{4\parallel}}{2}\rho_{r,s}(x)\rho_{r,s}(x) + \frac{g_{4\perp}}{2}\rho_{r,s}(x)\rho_{r,-s}(x) \right], \qquad (3.20)$$

$$H_2 = \int dx \sum_{s=\uparrow,\downarrow} \left[\frac{g_{2\parallel}}{2}\rho_{R,s}(x)\rho_{L,s}(x) + \frac{g_{2\perp}}{2}\rho_{R,s}(x)\rho_{L,-s}(x) \right], \qquad (3.21)$$

In order to diagonalise the Hamiltonian, we define the following bosonic fields

$$\phi_\rho(x) = \frac{1}{\sqrt{2}}[\phi_\uparrow + \phi_\downarrow],$$
$$\phi_\sigma(x) = \frac{1}{\sqrt{2}}[\phi_\uparrow - \phi_\downarrow], \qquad (3.22)$$

with charge and spin density defined as

$$\rho(x) = \frac{1}{\sqrt{2}}[\rho_\uparrow(x) + \rho_\downarrow(x)],$$
$$\sigma(x) = \frac{1}{\sqrt{2}}[\rho_\uparrow(x) - \rho_\downarrow(x)]. \qquad (3.23)$$

Apparently, the ρ and σ fields commute with each other and have the usual bosonic commutation relations (cf. Eq. 3.17) among themselves. The fermionic field operator is

$$\psi_{r,s} = \frac{1}{\sqrt{2\pi a}}F_{r,s}e^{irk_F x}e^{-\frac{i}{\sqrt{2}}[r\phi_\rho(x)-\theta_\rho(x)+s(r\phi_\sigma(x)-\theta_\sigma(x))]}. \qquad (3.24)$$

Hence, we can rewrite the interaction Hamiltonians 3.20, 3.21 in terms of the redefined bosonic fields,

$$
\begin{aligned}
H_4 = \frac{1}{4\pi^2} \int dx (g_{4\parallel} + g_{4\perp}) &[(\nabla\phi_\rho(x))^2 + (\nabla\theta_\rho(x))^2] \\
&+ (g_{4\parallel} - g_{4\perp})[(\nabla\phi_\sigma(x))^2 + (\nabla\theta_\sigma(x))^2].
\end{aligned}
\tag{3.25}
$$

$$
\begin{aligned}
H_2 = \frac{1}{4\pi^2} \int dx (g_{2\parallel} + g_{2\perp}) &[(\nabla\phi_\rho(x))^2 - (\nabla\theta_\rho(x))^2] \\
&+ (g_{2\parallel} - g_{2\perp})[(\nabla\phi_\sigma(x))^2 - (\nabla\theta_\sigma(x))^2].
\end{aligned}
\tag{3.26}
$$

The g_1 process is slightly more difficult to deal with. $g_{1\parallel}$ term is the same as $g_{2\parallel}$ term after permutating the fermionic operators, but $g_{1\perp}$ term behaves very differently, namely

$$
\begin{aligned}
H_1 &= \int dx g_{1\parallel} \sum_s [\psi_{L,s}^\dagger \psi_{R,s}^\dagger \psi_{L,s} \psi_{R,s}] + g_{1\perp} \sum_s [\psi_{L,s}^\dagger \psi_{R,-s}^\dagger \psi_{L,-s} \psi_{R,s}] \\
&= \int dx - g_{1\parallel} \sum_s [\psi_{L,s}^\dagger \psi_{L,s} \psi_{R,s}^\dagger \psi_{R,s}] + g_{1\perp} \sum_s [\psi_{L,s}^\dagger \psi_{R,s} \psi_{R,-s}^\dagger \psi_{L,-s}] \\
&= \int dx - g_{1\parallel} \sum_s [\rho_{L,s} \rho_{R,s}] + \frac{g_{1\perp}}{(2\pi a)^2} \sum_s [e^{i(-2\phi_s)} e^{i(2\phi_{-s})}].
\end{aligned}
\tag{3.27}
$$

Specifically for the anomalous $g_{1\perp}$ term, using Eq. 3.22, $g_{1\perp}$ term becomes

$$
H_{1\perp} = \int dx \frac{g_{1\perp}}{(2\pi a)^2} (e^{2\sqrt{2}\phi_\sigma} + e^{-2\sqrt{2}\phi_\sigma}) = \int dx \frac{2g_{1\perp}}{(2\pi a)^2} \cos(2\sqrt{2}\phi_\sigma(x)).
\tag{3.28}
$$

Combining the free Hamiltonian and all the interaction terms, we obtain the full Hamiltonian

$$
H = H_\rho + H_\sigma,
\tag{3.29}
$$

$$
\begin{aligned}
H_\rho &= \frac{u_\rho}{2\pi} \int dx \left[K_\rho(\nabla\theta_\rho(x))^2 + \frac{1}{K_\rho}(\nabla\phi_\rho(x))^2 \right], \\
H_\sigma &= \frac{u_\sigma}{2\pi} \int dx \left[K_\sigma(\nabla\theta_\sigma(x))^2 + \frac{1}{K_\sigma}(\nabla\phi_\sigma(x))^2 \right] + \frac{2g_{1\perp}}{(2\pi a)^2} \cos(2\sqrt{2}\phi_\sigma(x)),
\end{aligned}
\tag{3.30}
$$

with renormalised coefficients (e.g. renormalised Fermi velocities u_ρ, u_σ, and renor-

malised Luttinger coefficients K_ρ, K_σ)

$$
\begin{aligned}
u_\rho &= v_F\sqrt{(1 + y_{4\rho}/2)^2 - (y_\rho/2)^2}, \\
u_\sigma &= v_F\sqrt{(1 + y_{4\sigma}/2)^2 - (y_\sigma/2)^2}, \\
K_\rho &= \sqrt{\frac{1 + y_{4\rho}/2 + y_\rho/2}{1 + y_{4\rho}/2 - y_\rho/2}}, \\
K_\sigma &= \sqrt{\frac{1 + y_{4\sigma}/2 + y_\sigma/2}{1 + y_{4\sigma}/2 - y_\sigma/2}}, \\
g_\rho &= g_{1\parallel} - g_{2\parallel} - g_{2\perp}, y_\rho = \frac{g_\rho}{\pi v_F}, \\
g_{4\rho} &= g_{4\parallel} + g_{4\perp}, y_{4\rho} = \frac{g_{4\rho}}{\pi v_F}, \\
g_\sigma &= g_{1\parallel} - g_{2\parallel} + g_{2\perp}, y_\sigma = \frac{g_\sigma}{\pi v_F}, \\
g_{4\sigma} &= g_{4\parallel} - g_{4\perp}, y_{4\sigma} = \frac{g_{4\sigma}}{\pi v_F}.
\end{aligned}
\tag{3.31}
$$

This is the celebrated Luttinger liquid theory for 1D spinful fermions. The significant meaning of writing the fermionic Hamiltonian in terms of bosonic field is that it is very obvious in bosonic language to observe the separation of charge (ρ) and spin (σ) parts. This phenomenon has important applications, i.e. one can obtain bona fide excitations from the 2 separate parts of Hamiltonian, namely holon for charge part, and spinon for spin part. This has been confirmed via experiments, and charge-spin separation is unique for 1D physics, too. Another interesting fact is that the spin part of Hamiltonian (H_σ) is a sine-Gordon equation. In the long-wavelength limit, it can end up with a spin gap, resulting in the Luther-Emery liquid, with the prediction of electron-pairing nature [26].

A more thorough summary of numerous bosonisation formulae is available in the Appendix A, which can be used as a supplement material for this thesis.

3.2 Density matrix renormalisation group

Density matrix renormalisation group (DMRG) is a numerical method to approximate the ground states and energy spectra of a physical systems. It has been invented in 1990s by Steven White [27, 28], and it becomes more powerful and one of the most important tools to analyse 1D systems after being rewritten systematically in matrix

product state (MPS) language [28, 29]. We will focus on the MPS description of DMRG in this thesis.

3.2.1 Matrix product states

MPS description characterises quantum states in terms of matrices. To be more specific, for an arbitrary quantum state $|\psi\rangle$ (in a lattice, here 1D lattice specifically), one can write it as

$$|\psi\rangle = \sum_{n_1, n_2, \cdots n_N} A_1^{n_1} A_2^{n_2} A_3^{n_3} \cdots A_N^{n_N} |n_1, n_2, n_3, \cdots n_N\rangle, \qquad (3.32)$$

where $A_i^{n_i}$ is a $d_{i-1} \times d_i$ matrix (note that $A_1^{n_1}$ is a $1 \times d_1$ matrix, and $A_N^{n_N}$ is a $d_{N-1} \times 1$ matrix), and n_1, n_2, ... n_N are the physical variables (e.g. for spin-1/2 systems, physical variables are local spin-1/2s), as shown in Fig. 3.3.
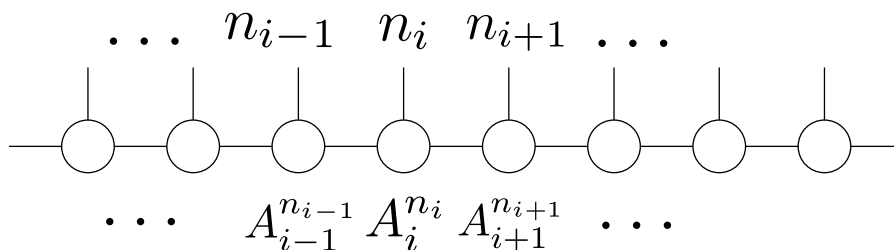
Figure 3.3: A typical MPS. $A_i^{n_i}$ is matrix corresponding to physical site i with physical variable n_i.

The dimensions of matrices A are called bond dimensions. The bond dimension is actually related to the entanglement structure among different physical variables, i.e. bigger the bond dimension is, more entangled the quantum state is. A trivial product state is not entangled, e.g. the ferromagnetic ground state of 1D Ising model $|\psi\rangle = |\uparrow\uparrow\uparrow \cdots\rangle$, and immediately we can get the bond dimension is 1, i.e. the state is not entangled at all.

Generically speaking, the bond dimension grows as the size of the physical system increases. This is so called "volume law", namely the bond dimension (entanglement of the system) is proportional to the volume of the physical system, e.g. linear dependence in the case of 1D. That intrinsically make it difficult to develop a numerical algorithm to approximate a state using MPS description. Fortunately, for a 1D gapped Hamiltonian,

the ground state's entanglement follows "area law" rather than the generic "volume law" [30, 31], i.e. the bond dimension (entanglement of the system) is proportional to the area of the physical system (the derivative of the volume). For example, the required bond dimension to approximate ground state(s) of 1D gapped Hamiltonian is a constant, leaving a possibility of efficiently determine the ground state(s) of 1D gapped Hamiltonian in terms of MPS.

DMRG can efficiently obtain the matrices $A_i^{n_i}$ by iterating the calculation of the energy eigenstates of Hamiltonian, approximating the ground state(s). In addition, by setting the bond dimension to a constant (in a translational invariant system), it is possible to calculate the error by calculating the trace of the density matrix $\mathrm{Tr}\,|\psi\rangle\langle\psi| - 1$, which helps us to determine the validity of DMRG method. More detailed explanations of the mechanism of DMRG algorithm are available in [28, 32] and reference therein.

In principle, people are also interested in physical systems in higher dimensions, or 1D gapless systems. The "area law" for higher dimensional Hamiltonian has not been rigorously proven, but there are some numerical evidences [33]. As for the 1D gapless systems, usually between second-order phase transition, it has been proven that the entanglement (measured by entanglement entropy, which will be explained in the later section) has a logarithm correction in addition to the "area law" [34, 35, 36]. There exist other DMRG algorithms for 2 or higher dimensions, or critical 1D systems, but we will ignore the discussion here.

3.2.2 Entanglement spectrum

One of the virtues of utilising DMRG to calculate the ground state(s) of 1D gapped Hamiltonian is that one can obtain the entanglement spectra of the ground state(s) easily, revealing useful (and usually non-local) information of the physical system.
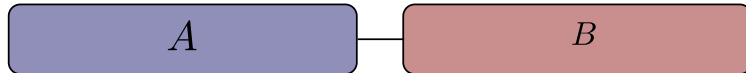
Figure 3.4: Division of two subsystems A and B in a 1D gapped system. After the division, one can calculate the entanglement between the two subsystems.

First of all, let us consider a 1D gapped system divided into two subsystems A and B, as shown in Fig. 3.4. We can define a reduced density matrix ρ_A for a pure state $|\psi\rangle$ as

$$\rho_A = \text{Tr}_B \rho = \text{Tr}_B |\psi\rangle \langle \psi|, \tag{3.33}$$

where Tr_B is the partial trace of subsystem B, i.e. $\text{Tr}_B |\psi\rangle \langle \psi| = \sum_b \langle b_B|\psi\rangle \langle \psi|b_B\rangle$, and $\{|b_B\rangle\}$ is a complete set of eigenstates of subsystem B.

Moreover, the pure state $|\psi\rangle$ can be rewritten in terms of the eigenstates of the two subsystems [36],

$$|\psi\rangle = \sum_{a,b} c_{a,b} |a_A\rangle |b_B\rangle, \tag{3.34}$$

where matrix entries $c_{a,b}$ is not necessarily diagonal. In addition, we can operate a Schmidt decomposition by finding orthonormal bases for subsystems A, B, i.e.

$$|\psi\rangle = \sum_{i=1}^{n_s} \alpha_i |\phi_i^A\rangle |\phi_i^B\rangle, \tag{3.35}$$

where n_s is the dimension of larger Hilbert space of subsystems A and B. α_i is called Schmidt eigenvalues, satisfying $\sum_i |\alpha_i|^2 = 1$. Hence the reduced density matrix ρ_A can be expressed as

$$\begin{aligned}
\rho_A &= \sum_b \langle b_B|\psi\rangle \langle \psi|b_B\rangle \\
&= \sum_{i=1}^{n_s} |\alpha_i|^2 |\phi_i^A\rangle \langle \phi_i^A| \\
&= \sum_{i=1}^{n_s} \lambda_i |\phi_i^A\rangle \langle \phi_i^A|,
\end{aligned} \tag{3.36}$$

with $\sum_i \lambda_i = 1$. One can do the similar calculation for subsystem B, and one can obtain

$$\rho_B = \text{Tr}_A |\psi\rangle \langle \psi| = \sum_{i=1}^{n_s} \lambda_i |\phi_i^B\rangle \langle \phi_i^B|. \tag{3.37}$$

Naïvely speaking, more entangled subsystems A and B are, more mixed the reduced density matrices are. For example, for a product state (i.e. not entangled at all), the reduced density matrices are still a pure state. From reduced density matrices ρ_A and ρ_B, it is natural to define a quantity to measure the entanglement between the two subsystems, i.e. entanglement entropy

$$S_A = -\text{Tr}\left(\rho_A \log \rho_A\right) = -\sum_{i=1}^{n_s} \lambda_i \log \lambda_i = -\text{Tr}\left(\rho_B \log \rho_B\right) = S_B. \tag{3.38}$$

As we have discussed beforehand, the ground state(s) of 1D gapped Hamiltonian follow "area law", i.e. the entanglement entropy is a constant. Indeed, entanglement entropy not only can tell us how entangled the two subsystems are, but also the topological properties of the state (so called topological entanglement entropy, more detailed explanation in [32, 36, 37, 38]).

In addition to entanglement entropy, one can also define entanglement spectrum [39], which can reveal more information about the quantum state. From the Schmidt decomposition of the reduced density matrices, one can define entanglement spectrum ξ_i as

$$|\psi\rangle = \sum_{i=1}^{n_s} \alpha_i |\phi_i^A\rangle |\phi_i^B\rangle = \sum_{i=1}^{n_s} e^{-\frac{1}{2}\xi_i} |\phi_i^A\rangle |\phi_i^B\rangle, \quad (3.39)$$
$$\lambda_i = e^{-\xi_i}.$$

The entanglement spectrum can be understood as the eigenvalues of an emergent "entanglement Hamiltonian" K_A defined as

$$K_A = -\log \rho_A. \quad (3.40)$$

Indeed, the entanglement spectrum is a nonlocal quantity of the physical system, thus it can reveal much useful information, e.g. the ground state degeneracy is the same as the degeneracy of entanglement spectrum eigenstates ξ_i of the ground state. This is extremely significant, because for some 1D SPT systems, it is intrinsically impossible to define a local order parameter, difficult to define a non-local one, but with the help of entanglement spectrum, one can easily obtain the ground state degeneracy, even identify different phases.

There is one important aspect of entanglement spectrum, which is that the choice of Schmidt decomposition could in principle change the degeneracy of the entanglement spectrum but not the physical ground state degeneracy, as discussed in [40]. We will not go into details on this issue, because within the scope of this thesis, it is not important, but in general it is significant to take into account this aspect.

3.3 Matrix product states and the protecting symmetries of SPT

Because of the area law of entanglement, the SPT phase appearing in the ground state(s) of certain 1D gapped systems should also be described faithfully via MPS.

In fact, from the MPS structure of states with SPT phase, one can determine which symmetries are important to protect the phase (or the ground state degeneracy).

Without losing generality, we assume that the systems we study are translationally invariant, e.g. with periodic boundary condition. A more general case can be shown with similar approach. We start with a translationally invariant MPS with N sites (Fig. 3.5)

$$|\psi\rangle = \sum_{\mathbf{n}} \text{Tr} \left(\cdots \Gamma^{n_i} \Lambda \Gamma^{n_{i+1}} \Lambda \cdots \right) |n_1, n_2, \cdots n_N\rangle, \tag{3.41}$$

where n_i are physical indices, and Λ is a real, diagonal matrix with non-negative elements [7, 41].
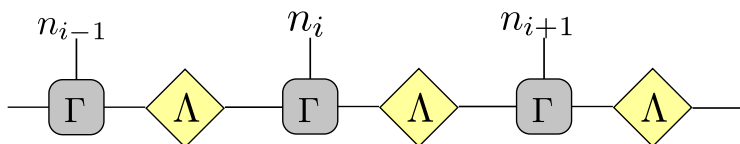
Figure 3.5: A generic translationally invariant MPS in Eq. 3.41.

The normalisation of MPS is given as

$$\sum_n \Gamma^n \Lambda^2 (\Gamma^n)^\dagger = \sum_n (\Gamma^n)^\dagger \Lambda^2 \Gamma^n = \mathbb{1}. \tag{3.42}$$

Assume that both Hamiltonian and ground state (Eq. 3.41) have the same (global) symmetry U, i.e. no spontaneous symmetry breaking, then

$$[H, U] = 0, \ U |\psi\rangle = e^{i\theta} |\psi\rangle. \tag{3.43}$$

If the symmetry can be written in local on-site terms, the symmetry of the physical indices can be transformed into the symmetry in the bonds (virtual dimensions) up to a phase (i.e. projective representation) [7, 8, 41], as shown in Fig. 3.6,

$$\sum_{n'} U^{nn'} \Gamma^{n'} = e^{i\theta_U} V^\dagger \Gamma^n V, \tag{3.44}$$
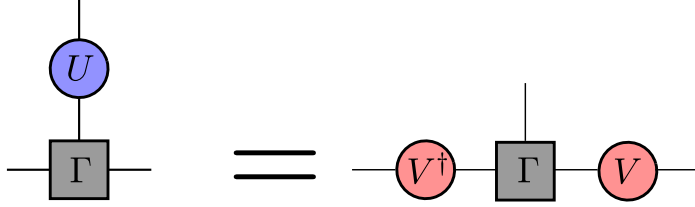
Figure 3.6: A local on-site symmetry operation on MPS is equivalent to a projective symmetry operation on the virtue bonds of MPS.

We will discuss several symmetries that could protect non-trivial SPT phases in spin-1 systems.

3.3.1 Inversion symmetry

Firstly, we look at how inversion symmetry acts on a MPS. Note that inversion symmetry cannot be written as local on-site terms. The transformation law of inversion symmetry U_I is

$$
\begin{aligned}
(\Gamma^n)^T &= e^{i\theta_I} V_I^\dagger \Gamma^n V_I, \\
\Gamma^n &= e^{2i\theta_I} (V_I V_I^*)^\dagger \Gamma^n (V_I V_I^*).
\end{aligned}
\tag{3.45}
$$

where $\theta_I \in [0, 2\pi)$ and V_I is a unitary operator acting on the virtual dimensions.

Use Eq. 3.42 and $[V_I, \Lambda] = 0$, we can obtain

$$
\sum_n \Gamma^n \Lambda (V_I V_I^*) \Lambda (\Gamma^n)^\dagger = e^{-2i\theta_I} V_I V_I^*,
\tag{3.46}
$$

and from Eq. 3.42, $e^{2i\theta_I} = 1$ and $V_I V_I^* = e^{i\phi_I} \mathbb{1}$. Since V_I is a unitary operator, it is equivalent to $V_I = e^{2\phi_I} V_I$, and thus $\phi_I = 0$ or π. Here we use an example that will be explained more in details in Chapter 4 to demonstrate that $\theta_I = \pi$ and $\phi_I = \pi$ corresponds to a non-trivial SPT phase. For AKLT ground state, which is in Haldane phase (SPT phase), $\Gamma^n = \sigma^n$, $\Lambda \propto \mathbb{1}$, where $n = +/0/-$ corresponds to a physical spin-1. Hence, $V_I = \sigma^y$, $\theta_I = \pi$, because $(\sigma^n)^T = -\sigma^y \sigma^n \sigma^y$. Moreover, $\sigma^y \sigma^{y*} = -\mathbb{1}$, i.e. $\phi_I = \pi$. The physical system is in SPT phase if $\theta_I = \pi$ and $\phi_I = \pi$, otherwise in trivial phase. Another important point is that the inversion symmetry has to be bond-centered, otherwise the site in the centre has an ambiguity of deciding the two

phases [7]. It elucidates that the bond-centered inversion symmetry can protect SPT phases.

3.3.2 Time reversal symmetry

For the convenience of the later part of the thesis, we restrict our discussion to time reversal symmetry of spin-1, i.e. $T = \prod_j U_{Tj} K = \prod_j e^{i\pi S_j^y} K$, where K is the complex conjugation operator. It essentially change $S^{x,y,z}$ to $-S^{x,y,z}$, and can be written into local on-site terms $U_{Ti} = e^{i\pi S_j^y}$.

In MPS description, from Eq. 3.44, Γ matrices transform as

$$\sum_{n'} U_T^{nn'} \Gamma^{n'*} = e^{i\theta_T} V_T^\dagger \Gamma^n V_T. \tag{3.47}$$

With similar method for inversion symmetry, one can obtain

$$\sum_n \Gamma^n \Lambda (V_T V_T^*) \Lambda (\Gamma^n)^\dagger = V_T V_T^*, \tag{3.48}$$

i.e. $V_T V_T^* = e^{i\phi_T} \mathbb{1}$, implying $\phi_T = 0$ or π. In conclusion, the SPT phase corresponds to $\phi_T = \pi$ and trivial phase corresponds to $\phi_T = 0$.

3.3.3 D_2 symmetry

Dihedral group D_2 (also called as $\mathbb{Z}_2 \times \mathbb{Z}_2$) consists of π rotation along x and z direction for spin-1 systems, denoting as R_x and R_z, respectively. (π rotation along y direction can be generated by $R_x R_z$.)

$$\begin{aligned} R_x &= \exp\left(i\pi S^x\right) \\ R_z &= \exp\left(i\pi S^z\right), \end{aligned} \tag{3.49}$$

$$\begin{aligned} n' R_x^{nn'} \Gamma^{n'*} &= e^{i\theta_x} V_x^\dagger \Gamma^n V_x \\ n' R_z^{nn'} \Gamma^{n'*} &= e^{i\theta_z} V_z^\dagger \Gamma^n V_z. \end{aligned} \tag{3.50}$$

It can be proved using similar method above that $V_x^2 = e^{i\phi_x} \mathbb{1}$, $V_z^2 = e^{i\phi_z} \mathbb{1}$ and $V_x V_z = e^{i\phi_{xz}} V_z V_x$. We obtain two possible values of ϕ_{xz} to be 0 or π. Similar situation happens, as system is in SPT phase if $\phi_{xz} = \pi$, and trivial if $\phi_{xz} = 0$.

More generally, if a symmetry (represented by a finite group or compact Lie group) has non-trivial projective representation, it can protect SPT phase(s), and the number

of possible SPT phases is given by the second cohomology group $H^2(G, \mathbb{C})$ of group G [9, 42, 43]. The most notable example would be $SO(3)$ symmetry, i.e.

$$H^2(SO(3), \mathbb{C}) = \mathbb{Z}_2, \tag{3.51}$$

two phases can be constructed with $SO(3)$ symmetry and one of them is a SPT phase. This is the case of AKLT ground states, which will be explained more in details.

More importantly, whether a symmetry protects SPT phase can be checked numerically by adding perturbation that breaks the specific symmetry and probing the ground state degeneracy via entanglement spectrum [7, 8].

Chapter 4

AKLT model

We investigate AKLT model, i.e. a toy model with short-range interaction exhibiting Haldane phase, in this chapter. AKLT model can be derived elegantly via parent Hamiltonian approach, which will be explained in the first part of this chapter. An important reason to investigate AKLT model is that we can express the ground states of AKLT Hamiltonian exactly by virtue of MPS description. The exact form of ground states makes the analytic calculation of correlation functions possible, predicting the existence of two localised edge states, and we express the edge mode operators by construction using the properties of ground states.

4.1 Parent Hamiltonian approach

In order to obtain the AKLT Hamiltonian, we use a different approach, namely writing down the ground states first, then constructing the Hamiltonian with the same ground states.

Firstly, we consider a dimerised spin-$\frac{1}{2}$ state with periodic boundary condition (PBC), which is unique, as demonstrated in Fig. 4.1. The dimers between two adjacent spin-$\frac{1}{2}$s are spin singlet ($\frac{1}{\sqrt{2}}(|\uparrow\downarrow\rangle - |\downarrow\uparrow\rangle)$).
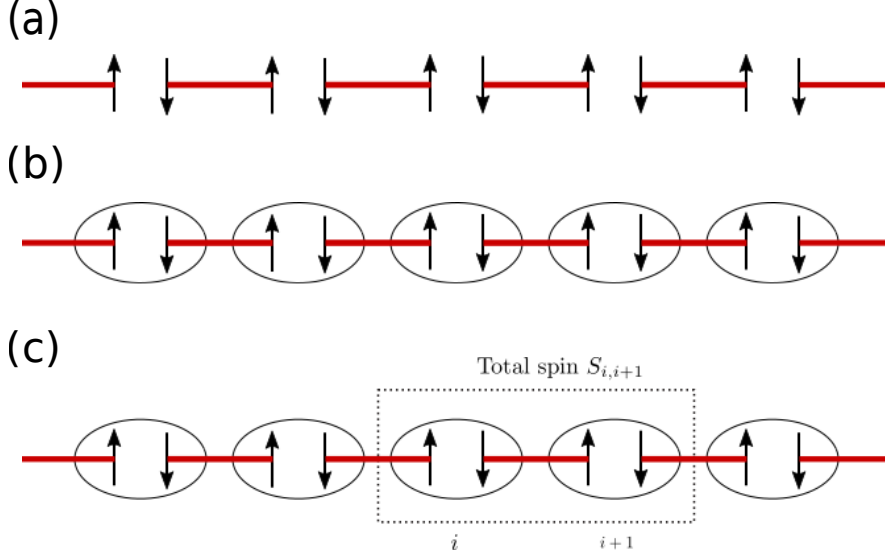
Figure 4.1: (a) A dimerised spin-$\frac{1}{2}$ chain. (b) The ground state of AKLT model. The eclipses over two adjacent spin-$\frac{1}{2}$s corresponds to a projection to spin-1 Hilbert subspace, i.e. $P^{S=1}|\psi\rangle$. (c) A projection of two adjacent spin-1s in AKLT ground state.

Then we project the adjacent spin-$\frac{1}{2}$s that do not form a dimer between each other into a spin-1 Hilbert subspace, as shown in Fig. 4.1. Originally two spin-$\frac{1}{2}$s have a 4 dimensional Hilbert space, and after the mapping, local Hilbert space has become 3 dimensional. By this construction, we obtain the ground state of AKLT model (with PBC).

After the projection, the spin singlets are damaged. The reason is that spin singlet is a maximally entangled state between two spins. If they are also correlated with other spin (in this case, projected with another spin), spin singlet will no longer remain exact. In addition, with the current setup, by working out the spin summation via Clebsch-Gordan coefficient, one can find out that for two adjacent spin-1s S_i, S_{i+1}, the total spin of two spin-1s $S_{i,i+1}$ is always smaller than 2 (cf. Fig. 4.1).

We know that for two spin-1s, the total spin lives in a Hilbert space as

$$1 \otimes 1 = 0 \oplus 1 \oplus 2, \tag{4.1}$$

consisting of a subspace of total spin 0, 1, and 2.

Hence, if the state we construct above is a ground state of a parent Hamiltonian, the parent Hamiltonian must be proportional to spin-2 projector $P_{i,i+1}^{S=2}$, i.e.

$$
\begin{aligned}
P_{i,i+1}^{S=2} &= \frac{1}{24}(\mathbf{S}_i + \mathbf{S}_{i+1})^2 \left[(\mathbf{S}_i + \mathbf{S}_{i+1})^2 - 2 \right] \\
&= \frac{1}{24}(4 + 2\mathbf{S}_i \cdot \mathbf{S}_{i+1})(2 + 2\mathbf{S}_i \cdot \mathbf{S}_{i+1}) \\
&= \frac{1}{6}(\mathbf{S}_i \cdot \mathbf{S}_{i+1})^2 + \frac{1}{2}(\mathbf{S}_i \cdot \mathbf{S}_{i+1}) + \frac{1}{3}, \\
H_{AKLT} &\propto \sum_{i,i+1} P_{i,i+1}^{S=2}.
\end{aligned}
\tag{4.2}
$$

Without losing generality, we can express the AKLT Hamiltonian as

$$
H_{AKLT} = \sum_{i,i+1} (\mathbf{S}_i \cdot \mathbf{S}_{i+1}) + \frac{1}{3}(\mathbf{S}_i \cdot \mathbf{S}_{i+1})^2.
\tag{4.3}
$$

Thus, we derive the parent Hamiltonian of AKLT state. This method is generically used to find new toy models using the projectors. With similar construction, one can obtain many parent Hamiltonians from AKLT-like states, which could be in the same physical phase as some physically realistic models, shedding light into a different approach than solving ground states for some arbitrary Hamiltonians.

4.2 MPS description and correlation functions

More importantly, the ground state of AKLT Hamiltonian can be written in terms of MPS. This can be observed by the effective spin-$\frac{1}{2}$ picture, Fig. 4.1. In MPS language, we could express the two effective spin-$\frac{1}{2}$s as the matrices with bond dimension of 2. Actually, the configuration of the two effective spin-$\frac{1}{2}$s can uniquely determine the physical spin-1, hence, with bond dimension only 2, one can faithfully describe the ground state of AKLT Hamiltonian.
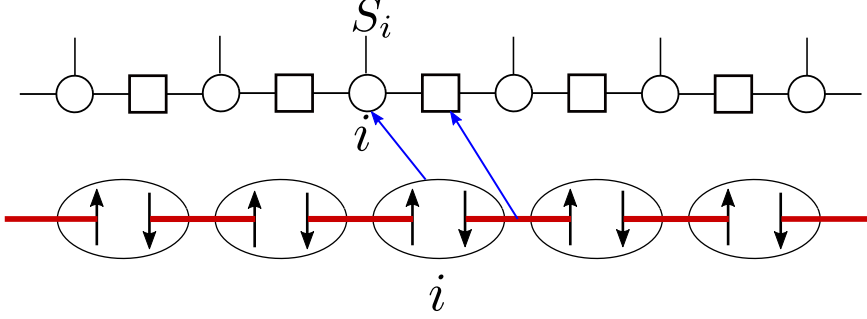
Figure 4.2: MPS description of AKLT ground state. The squares correspond to the spin singlet matrices $\Sigma_{b_i,a_{i+1}}$, while the circles correspond to the spin-1 projectors with physical spin indices S_i, i.e. $A^{S_i}_{a_i,b_i}$.

As described in Fig. 4.2, we can write down the MPS for AKLT ground state with PBC as

$$
\begin{aligned}
|\psi\rangle &= \sum_{\mathbf{S}} \sum_{a,b} A^{S_1}_{a_1,b_1} \Sigma_{b_1,a_2} A^{S_2}_{a_2,b_2} \Sigma_{b_2,a_3} \cdots A^{S_N}_{a_N,b_N} \Sigma_{b_N,a_1} |\mathbf{S}\rangle \\
&= \sum_{\mathbf{S}} \mathrm{Tr}(A^{S_1}\Sigma A^{S_2}\Sigma \cdots A^{S_N}\Sigma |\mathbf{S}\rangle),
\end{aligned}
\tag{4.4}
$$

where S_i is the physical spin of site i, and its values are $+1$ $(+)$, 0 and -1 $(-)$. a_i, b_i are the effective spin-$\frac{1}{2}$s. Spin singlet matrices $\Sigma_{b_i,a_{i+1}}$ and spin-1 projectors with physical spin indices S_i, i.e. $A^{S_i}_{a_i,b_i}$ are enough to describe the ground state. Therefore, we can obtain the matrices as

$$
\begin{aligned}
A^+ &= \begin{pmatrix} 1 & 0 \\ 0 & 0 \end{pmatrix}, A^0 = \begin{pmatrix} 0 & \frac{1}{\sqrt{2}} \\ \frac{1}{\sqrt{2}} & 0 \end{pmatrix}, A^- = \begin{pmatrix} 0 & 0 \\ 0 & 1 \end{pmatrix} \\
\Sigma &= \begin{pmatrix} 0 & \frac{1}{\sqrt{2}} \\ -\frac{1}{\sqrt{2}} & 0 \end{pmatrix}.
\end{aligned}
\tag{4.5}
$$

With PBC, we can combine the matrices $A^{S_i}\Sigma$ as a new set of matrices B^{S_i} with normalisation condition $\sum_S B^{S\dagger}B^S = \mathbb{1}$,

$$
B^+ = \begin{pmatrix} 0 & \sqrt{\frac{2}{3}} \\ 0 & 0 \end{pmatrix}, B^0 = \begin{pmatrix} -\frac{1}{\sqrt{3}} & 0 \\ 0 & \frac{1}{\sqrt{3}} \end{pmatrix}, B^- = \begin{pmatrix} 0 & 0 \\ -\sqrt{\frac{2}{3}} & 0 \end{pmatrix}.
\tag{4.6}
$$

We can now check the normalisation $\langle\psi|\psi\rangle$

$$\langle\psi|\psi\rangle = \sum_{\mathbf{S}} \text{Tr}(B^{S_1}B^{S_2}\cdots B^{S_N})^* \text{Tr}(B^{S_1}B^{S_2}\cdots B^{S_N})$$

$$= \text{Tr}\left(\sum_{S_1} B^{S_1*}\otimes B^{S_1}\right)\left(\sum_{S_2} B^{S_2*}\otimes B^{S_2}\right)\cdots\left(\sum_{S_N} B^{S_N*}\otimes B^{S_N}\right) = \text{Tr}E^N,$$

$$(4.7)$$

$$E = \sum_S B^{S*}\otimes B^S = \begin{pmatrix} \frac{1}{3} & 0 & 0 & \frac{2}{3} \\ 0 & -\frac{1}{3} & 0 & 0 \\ 0 & 0 & -\frac{1}{3} & 0 \\ \frac{2}{3} & 0 & 0 & \frac{1}{3}, \end{pmatrix} \tag{4.8}$$

by using the property of trace $\text{Tr}X \cdot \text{Tr}Y = \text{Tr}(X \otimes Y)$. One can easily find the eigenvalues of matrix E are 1, $-\frac{1}{3}$, $-\frac{1}{3}$, $-\frac{1}{3}$ by diagonalising the matrix [28], hence, the normalisation relation becomes

$$\langle\psi|\psi\rangle = 1 + 3\left(-\frac{1}{3}\right)^N \to 1, \tag{4.9}$$

if the system is in thermodynamic limit $N \to \infty$. The method also allows us to calculate the correlation functions in thermodynamic limit.

This can actually confirm the existence of a SPT phase in AKLT model, with the absence of local order parameter. For instance, $\langle S_i^z S_{i+r}^z\rangle$ can be calculated as

$$\langle S_i^z S_j^z\rangle = \text{Tr}\left(B^{+i*}\otimes B^{+i} + B^{-i*}\otimes B^{-i}\right)\left(\sum_{S_{i+1}} B^{S_{i+1}*}\otimes B^{S_{i+1}}\right)\cdots$$

$$\left(B^{+i+r*}\otimes B^{+i+r} + B^{-i+r*}\otimes B^{-i+r}\right)\cdots$$

$$= \text{Tr}(FE^{r-1}FE^{N-r-1}), \tag{4.10}$$

$$F = B^{+*}\otimes B^+ + B^{-*}\otimes B^- = \begin{pmatrix} 0 & 0 & 0 & \frac{2}{3} \\ 0 & 0 & 0 & 0 \\ 0 & 0 & 0 & 0 \\ -\frac{2}{3} & 0 & 0 & 0 \end{pmatrix}.$$

Eventually, one can get the 2-point correlation function $\langle S_i^z S_{i+r}^z\rangle$ decays exponentially as r increases, when the system approaches thermodynamic limit $(N \to \infty)$

$$\langle S_i^z S_{i+r}^z\rangle = \frac{4}{3}\left(-\frac{1}{3}\right)^r + \frac{4}{3}\left(-\frac{1}{3}\right)^{N-r} \to \frac{4}{3}\left(-\frac{1}{3}\right)^r, \tag{4.11}$$

indicating an energy gap between the ground state and excited states. More importantly, one can check similar 2-point correlation functions, e.g. $\langle S_i^+ S_{i+r}^-\rangle$, which are all

exponentially decaying, i.e. absence of local order parameters. The correlation length is $\log 3$, which we could use real space renormalisation group mapping to find a fix-point model for AKLT Hamiltonian with 0 correlation length. Furthermore, one can define a non-local order parameter (string order parameter) $\mathcal{O}$ as

$$\langle \mathcal{O} \rangle = \langle S_i^z \exp\left(i\pi \sum_{i<k<j} S_k^z\right) S_j^z \rangle = -\frac{4}{9} - 4\left(\frac{1}{3}\right)^N \to -\frac{4}{9}, \tag{4.12}$$

the expectation value of $\mathcal{O}$ goes to $-\frac{4}{9}$, as approaching to thermodynamic limit $N \to \infty$. The existence of non-vanishing string order parameter is a strong indication of SPT phase in 1D, albeit it is not always possible to define a string order parameter for SPT phases (especially in higher dimensions).

The existence of SPT phase also implies that in open boundary condition (OBC), the ground state degeneracy will increase. This is indeed the case for AKLT ground state, and it is easy to observe by means of MPS description. For OBC, we obtain four degenerate ground states

$$|\uparrow \cdots \uparrow\rangle, \ |\uparrow \cdots \downarrow\rangle, \ |\downarrow \cdots \uparrow\rangle, \ |\downarrow \cdots \downarrow\rangle, \tag{4.13}$$

where $\uparrow$ and $\downarrow$ represent the effective edge spin-$\frac{1}{2}$s in Fig. 4.3.
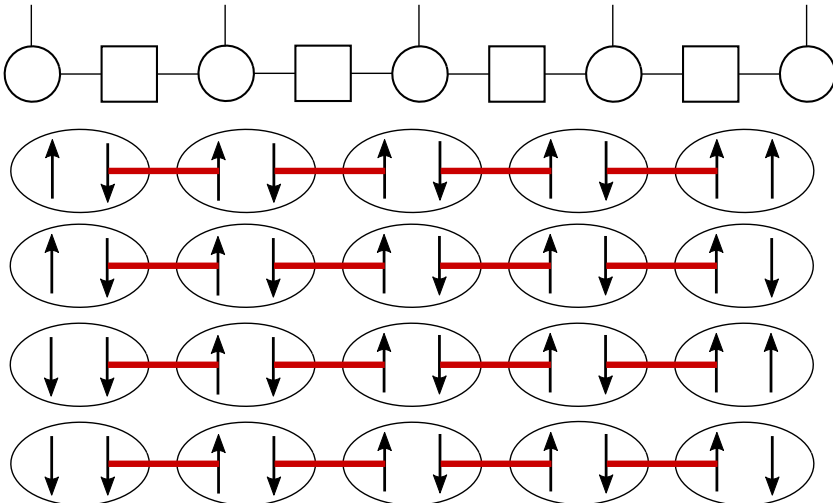
Figure 4.3: Ground states of AKLT model in OBC. Depending on the edge spin-$\frac{1}{2}$s, we can obtain 4 degenerate ground states, as a consequence of symmetry fractionalisation.

In addition, we can write down the 4 OBC ground states in terms of MPS. As shown in Fig. 4.3, the right edge is now different from the PBC case, with one Σ matrix missing. Indeed, in thermodynamic limit, we obtain

$$
\begin{aligned}
|\uparrow \cdots \uparrow\rangle &= \sum_{\mathbf{S}} \sum_{\mathbf{a}} B_{\uparrow a_2}^{S_1} B_{a_2 a_3}^{S_2} \cdots B_{a_{N-1} a_N}^{S_{N-1}} A_{a_N \uparrow}^{S_N} |S_1, S_2 \cdots S_N\rangle, \\
|\uparrow \cdots \downarrow\rangle &= \sum_{\mathbf{S}} \sum_{\mathbf{a}} B_{\uparrow a_2}^{S_1} B_{a_2 a_3}^{S_2} \cdots B_{a_{N-1} a_N}^{S_{N-1}} A_{a_N \downarrow}^{S_N} |S_1, S_2 \cdots S_N\rangle, \\
|\downarrow \cdots \uparrow\rangle &= \sum_{\mathbf{S}} \sum_{\mathbf{a}} B_{\downarrow a_2}^{S_1} B_{a_2 a_3}^{S_2} \cdots B_{a_{N-1} a_N}^{S_{N-1}} A_{a_N \uparrow}^{S_N} |S_1, S_2 \cdots S_N\rangle, \\
|\downarrow \cdots \downarrow\rangle &= \sum_{\mathbf{S}} \sum_{\mathbf{a}} B_{\downarrow a_2}^{S_1} B_{a_2 a_3}^{S_2} \cdots B_{a_{N-1} a_N}^{S_{N-1}} A_{a_N \downarrow}^{S_N} |S_1, S_2 \cdots S_N\rangle,
\end{aligned}
\tag{4.14}
$$

where A and B matrices are given in Eq. 4.5 and 4.6.

An important observation is that the physical system has finite size effect with OBC. This can be seen as an energy split between $S_{total} = 0$ and $S_{total} = 1$ sectors within the ground state manifold by calculating the energy spectrum of the AKLT chain. As shown in Fig. 4.4, the energy split between the states decays exponentially, predicting a true fourfold ground state degeneracy in thermodynamic limit.
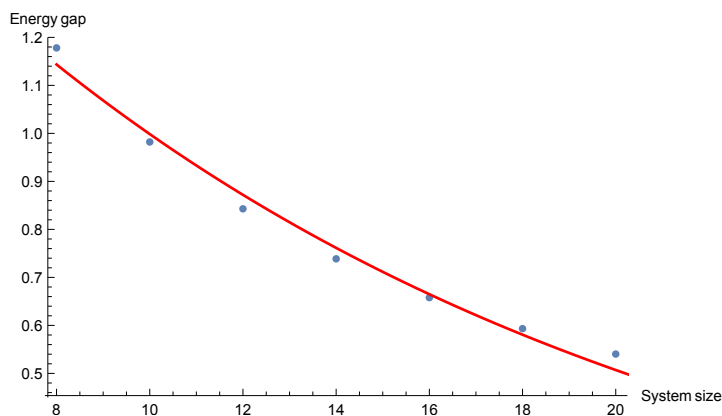
Figure 4.4: The finite size correction on the energy split between ground states (with unit of J). The red curve is the fitting of the energy split with respect of total length of the system with exponential function.

4.3 Symmetries that protect Haldane phase

As we have discussed in the previous sections, the symmetries that protect SPT phase must have non-trivial projective representation. From the criterion, we can find the

symmetries that protect Haldane phase in AKLT model.

In AKLT Hamiltonian 4.3, we can find a global $SO(3)$ symmetry. Due to the fact that $SU(2)$ is the double cover of $SO(3)$, i.e. $SO(3) \cong SU(2)/\mathbb{Z}_2$, we could conclude that $SU(2)$ is a non-trivial projective representation of $SO(3)$ (cf. Eq. 3.51).

As well as time-reversal symmetry and bond-centered inversion symmetry as analysed in Section 3.3, we obtain 3 symmetries that AKLT model has and have non-trivial projective representation. Therefore, the Haldane phase appeared in the ground states of AKLT model is protected by global $SO(3)$, time reversal and bond-centered inversion symmetry. And the Haldane phase exists as long as the perturbations do not break all 3 symmetries.
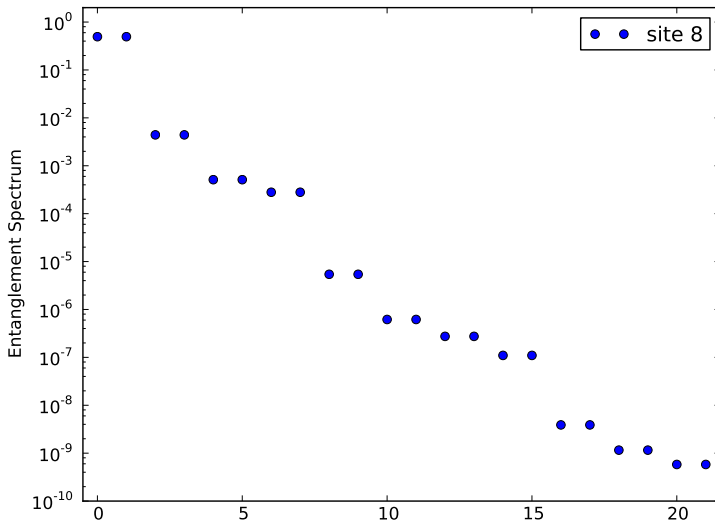
Figure 4.5: Entanglement spectrum of AKLT model with site $L = 16$. Due to the finite size correction, there is a energy gap between $S = 0$ and $S = 1$. The degeneracy in the figure represents the degeneracy of ground state submaniford $|\sum S^z| = 1$.

4.4 Hidden symmetry breaking

In spite of the absence of local order parameter, the SPT phase in AKLT ground states can be transformed to a symmetry breaking phase via a non-local unitary transformation, Kennedy-Tasaki (KT) transformation [44, 45, 46]. This is also referred in many literatures as "hidden symmetry breaking" [47].

KT transformation is defined as

$$U_{KT} = \prod_{j<k} \exp\left(i\pi S_j^z S_k^x\right) \tag{4.15}$$

Hence, we obtain the spin operators after the transformation

$$
\begin{aligned}
U_{KT} S_j^x U_{KT}^\dagger &= S_j^x \prod_{k>j} \exp\left(i\pi S_k^x\right), \\
U_{KT} S_j^y U_{KT}^\dagger &= \prod_{k<j} \exp\left(i\pi S_k^z\right) S_j^y \prod_{k>j} \exp\left(i\pi S_k^x\right), \\
U_{KT} S_j^z U_{KT}^\dagger &= \prod_{k<j} \exp\left(i\pi S_k^z\right) S_j^z.
\end{aligned}
\tag{4.16}
$$

The transformed AKLT Hamiltonian is

$$
\begin{aligned}
H_{KT} &= H' + \frac{1}{3}\left(H'\right)^2, \\
H' &= \sum_j -S_j^x S_{j+1}^x + S_j^y \exp\left[i\pi(S_j^z + S_{j+1}^x)\right] - S_j^z S_{j+1}^z.
\end{aligned}
\tag{4.17}
$$

More interestingly, the non-vanishing string order parameter $\mathcal{O} = S_i^z \exp\left(i\pi \sum_{i<k<j} S_k^z\right) S_j^z$ has been transformed into a ferromagnetic order parameter $\mathcal{O}'$,

$$\mathcal{O}' = -U_{KT} \mathcal{O} U_{KT}^\dagger = S_j^z S_k^z. \tag{4.18}$$

Because the expectation value of the new ferromagnetic order parameter in the transformed basis is the same as the one of string order parameter in the original basis, i.e.

$$\langle \mathcal{O}' \rangle_{transformed} = -\langle \mathcal{O} \rangle_{original} \to \frac{4}{9}, \ |i-k| \to \infty. \tag{4.19}$$

Therefore, we obtain a non-vanishing ferromagnetic order parameter for the transformed Hamiltonian, indicating a spontaneous symmetry breaking of rotational symmetry. It looks quite odd initially, since we start from a SPT phase and end up with a symmetry breaking phase. The crucial point here is that a non-local unitary transformation can change the physics of the original model, by disentangling the entanglement between different sites (or vice versa) [48], and eventually we arrive at a model with the same energy spectrum but different phases. This also happens when one uses Jordan-Wigner transformation to transform a Kitaev chain (in fermionic SPT phase) to an Ising chain with transverse field (in $\mathbb{Z}_2$ symmetry breaking phase) [49].

The on-site $SO(3)$ symmetry of the original AKLT model is now highly non-local after the transformation. But there is a subgroup of the original $SO(3)$ symmetry group which remains the same, i.e. D_2 ($\mathbb{Z}_2 \times \mathbb{Z}_2$) group. D_2 group is a discrete group that can be generated by $R_x = \prod_j \exp{(i\pi S_j^x)}$ and $R_z = \prod_j \exp{(i\pi S_j^z)}$, i.e. global π rotation along x and z directions mentioned in Chapter 3.

$$\begin{aligned} U_{KT} \exp{(i\pi S_j^x)} U_{KT}^\dagger &= \exp{(i\pi S_j^x)}, \\ U_{KT} \exp{(i\pi S_j^z)} U_{KT}^\dagger &= \exp{(i\pi S_j^z)}. \end{aligned} \tag{4.20}$$

For the original AKLT Hamiltonian, $SO(3)$ symmetry cannot be broken spontaneously due to Mermin-Wagner theorem, i.e. global continuous symmetry acting locally cannot be broken simultaneously in quantum phase transition in 1D systems with only short-range interaction. But for the case of transformed Hamiltonian, most of the local terms of $SO(3)$ symmetry has been transformed into a highly non-local terms with continuous property hidden, but D_2 symmetry remains the same. Since D_2 symmetry is a discrete symmetry, we expect a D_2 symmetry breaking in a quantum phase transition in the transformed Hamiltonian.

From the analysis above, we could obtain the four ground states of the transformed Hamiltonian

$$\begin{aligned} |\text{GS}\rangle &= |\phi_i \phi_i \phi_i \phi_i \phi_i \cdots\rangle, i = 1, 2, 3, 4. \\ |\phi_1\rangle &= \frac{1}{\sqrt{3}}(|0\rangle + \sqrt{2}\,|+\rangle), |\phi_2\rangle = \frac{1}{\sqrt{3}}(|0\rangle - \sqrt{2}\,|+\rangle), \\ |\phi_3\rangle &= \frac{1}{\sqrt{3}}(|0\rangle + \sqrt{2}\,|-\rangle), |\phi_1\rangle = \frac{1}{\sqrt{3}}(|0\rangle - \sqrt{2}\,|-\rangle). \end{aligned} \tag{4.21}$$

Note that the four degenerate ground states of the transformed Hamiltonian do not correspond to the ground states of the original AKLT Hamiltonian given in Eq. 4.14 after transformation but superpositions of states within the ground state manifold. The ground state degeneracy remains the same in both original and transformed Hamiltonian, but the Haldane phase has become a symmetry breaking phase after KT transformation.

4.5 Edge modes in AKLT ground states

From Fig. 4.3, we would expect that there exist two edge states in AKLT chain, corresponding the 2 effective edge spin-$\frac{1}{2}$s. Firstly, we can take a look at AKLT ground

states described by MPS, and one distinct property is

$$B^+(B^0)^n B^+ = B^-(B^0)^n B^- = 0, \forall n \in \mathbb{Z}^+, \tag{4.22}$$

implying that $+1$ spin and -1 spin always come in pairs with 0 spins in between. Thus, we could depict the ground states of AKLT model in a pictorial way in Fig. 4.6.

Figure 4.6: A pictorial description of AKLT ground states in the bulk. $+$ and $-$ spins always appear in an alternating way, in between of 0 spins.

Moreover, for OBC, if the left edge has an effective spin-$\frac{1}{2}$ of up spin (or down spin), the first non-zero physical spin-1 would be $+$ (or $-$), and the argument works for the right edge too. From the observation above, we construct an edge mode operator that acts locally (i.e., with exponentially decaying expectation value)

$$\begin{aligned}
\Psi &= \Psi_1 + \Psi_2 + \Psi_3 + \cdots \\
\Psi_1 &= S_1^z, \Psi_2 = [\mathbb{1} - (S_1^z)^2]S_2^z, \cdots, \\
\Psi_n &= [\mathbb{1} - (S_1^z)^2][\mathbb{1} - (S_2^z)^2] \cdots [\mathbb{1} - (S_{n-1}^z)^2]S_n^z, \cdots
\end{aligned} \tag{4.23}$$

The expectation values can be calculated via MPS description of ground states at thermodynamic limit. For states with $|\uparrow \cdots\rangle$,

$$\begin{aligned}
\langle \Psi_1 \rangle &= \frac{2}{3}, \langle \Psi_2 \rangle = \frac{2}{9}, \cdots, \langle \Psi_n \rangle = \frac{2}{3^n}, \\
\langle \Psi \rangle &= \sum_n \langle \Psi_n \rangle = \frac{\frac{2}{3}(1 - \frac{1}{3^n})}{1 - \frac{1}{3}} \to 1.
\end{aligned} \tag{4.24}$$

It proves that the expectation values of higher order terms decay exponentially, i.e. the operator localises at the left edge. Meanwhile, for states with $|\downarrow \cdots\rangle$,

$$\begin{aligned}
\langle \Psi_1 \rangle &= -\frac{2}{3}, \langle \Psi_2 \rangle = -\frac{2}{9}, \cdots, \langle \Psi_n \rangle = -\frac{2}{3^n}, \\
\langle \Psi \rangle &= \sum_n \langle \Psi_n \rangle = -\frac{\frac{2}{3}(1 - \frac{1}{3^n})}{1 - \frac{1}{3}} \to -1.
\end{aligned} \tag{4.25}$$

Then we can check that the edge mode operator that we constructed can indeed change ground states within the ground state manifold,

$$\Psi \frac{1}{\sqrt{2}}(|\uparrow \cdots\rangle \pm |\uparrow \cdots\rangle) = \frac{1}{\sqrt{2}}(|\uparrow \cdots\rangle \mp |\uparrow \cdots\rangle). \tag{4.26}$$

The same approach can be applied for the right edge as well. We can define a right edge mode operator as

$$\begin{aligned}
\Psi' &= \Psi'_1 + \Psi'_2 + \Psi'_3 + \cdots \\
\Psi'_1 &= S^z_N, \Psi'_2 = [\mathbb{1} - (S^z_N)^2]S^z_{N-1}, \cdots, \\
\Psi'_n &= [\mathbb{1} - (S^z_N)^2][\mathbb{1} - (S^z_{N-1})^2]\cdots[\mathbb{1} - (S^z_{N-n+2})^2]S^z_{N-n+1}, \cdots
\end{aligned} \tag{4.27}$$

which satisfies similar properties as the left edge mode operator Ψ.

4.5.1 Classification of edge modes

Edge modes have drawn lots of attention, especially after the discovery of edge modes in Kitaev chain, which have non-Abelian statistics in quasi-1D systems [10, 11, 12, 13, 50]. It is natural to classify different edge modes appearing in different models. Here we concentrate on the classification proposed by Paul Fendley, so called "strong/weak edge mode" [49, 51, 52, 53, 54].

A strong edge mode S localised at one edge is defined with a quantum Hamiltonian H on a N-site chain with OBC as

- $[H, S] \to 0$ as $N \to \infty$, with finite-size correction decaying exponentially.

- $[S, D] \neq 0$, where D is a discrete symmetry of Hamiltonian H, i.e. $[H, D] = 0$, and $D^n = \mathbb{1}$, for certain positive integer n.

- $S^m \propto \mathbb{1}$, for certain positive integer m.

Meanwhile, a weak edge mode W localised at one edge is defined similarly, except for the first criterion, i.e.

- $[H, W]$ does not converge to 0 exponentially as the size $N \to \infty$.

- $[W, D] \neq 0$, where D is a discrete symmetry of Hamiltonian H, i.e. $[H, D] = 0$, and $D^n = \mathbb{1}$, for certain positive integer n.

- $W^m \propto \mathbb{1}$, for certain positive integer m.

The difference between strong and weak edge modes is that the strong edge mode commutes with the Hamiltonian (with exponentially small correction), and it guarantees that the degeneracy of states not only works for ground states but even for all excited states [49, 52, 53, 54], while the weak one only works within the ground state manifold (i.e. only ground state degeneracy is presented). This property of strong edge modes is referred as eigenstate phase transition [54]. For instance, assume a generic eigenstate of Hamiltonian H with a strong edge mode S (not necessarily a ground state), i.e. $H|a_1\rangle = E_a|a_1\rangle$, we can obtain a set of eigenstates $\{|a_i\rangle\}$ defined as

$$|a_i\rangle = S^{i-1}|a_1\rangle, \; i \in \mathbb{Z}^+, i \leq m, \tag{4.28}$$

where the set of eigenstates $\{|a_i\rangle\}$ are degenerate and orthogonal to each other

$$H|a_i\rangle = HS^{i-1}|a_1\rangle = S^{i-1}H|a_1\rangle = E_a|a_i\rangle,$$
$$\langle a_1|a_i\rangle = 0, \forall i \in \mathbb{Z}^+, i \leq m. \tag{4.29}$$

If an edge mode is strong, one can in principle use the degeneracy of excited states to encode quantum information as thermal states. (Note that the definition of strong/weak edge modes does not require the states to have topologically non-trivial phase.) For example, Kitaev chain in fermionic SPT phase has strong edge modes (hence also called strong zero mode, due to the fact that edge mode operator commutes with Hamiltonian, i.e. zero-energy excitation), as well as Ising chain with transverse field, i.e. dual to Kitaev chain via Jordan-Wigner transformation [55].

In the case of the edge modes Ψ and Ψ' we propose for AKLT ground states, they anticommute with discrete symmetry operators of D_2, $\Psi^2 = (\Psi')^2 = \mathbb{1}$, but they do not commute with the Hamiltonian, $[H, \Psi] \neq 0$, $[H, \Psi'] \neq 0$. Therefore, they are weak edge modes from the definition above. It is natural to ask whether a ground state of a 1D quantum Hamiltonian has strong edge mode(s). Unfortunately, we are not able to answer this question within the scope of this thesis, but we summarise the previous work on this topic:

- The models that have strong edge modes: Kitaev chain/Ising chain with transverse field, $\mathbb{Z}_3$ parafermion chain [49, 52, 53], interacting Majorana chain/spin-$\frac{1}{2}$ XYZ chain [54].

- Some models with strong edge modes can be mapped into dual models via a non-local unitary transformation, which have different physical properties but with the same energy spectra. The edge mode operators in each models remain local after the non-local unitary transformation.

- We find out that the known models with strong edge modes are all exactly solvable (integrable). We only find weak edge modes in AKLT model that is not exactly solvable, but it is possible to find a fixed-point model with the same SPT phase that is exactly solvable and has strong edge modes (more details explained later).

From the above summary, we conjecture that the existence of strong edge modes is related to the exact solvability of a many-body Hamiltonian.

4.5.2 Fixed-point model of AKLT Hamiltonian

As we know from the previous sections, one can construct two weak edge mode operators localised at each edge. The global $SO(3)$ symmetry fractionalises at the edges into $SU(2)$ symmetry locally at two edges, known as the "symmetry fractionalisation" phenomenon. In fact, we could use real space renormalisation group transformation method on the AKLT ground states [56], and eventually arrive at the fixed-point model of AKLT Hamiltonian with 0 correlation length. The method mentioned is sketched in Fig. 4.7. Firstly, we map two sites of the MPS of AKLT ground states into one site with one physical index after coarse-graining. In general, the physical Hilbert space of the new site would enlarge as Hilbert space of $1 \otimes 1$, but due to the fact that AKLT Hamiltonian $H_{AKLT} \propto \sum_{i,i+1} P_{i,i+1}^{S=2}$, the Hilbert space of new site just change from triplet into a singlet and a triplet ($\frac{1}{2} \otimes \frac{1}{2} = 0 \oplus 1$). In thermodynamic limit, we can perform this transformation for infinity times, and the local physical Hilbert space is always 4 dimensional after coarse graining. Eventually, the model's correlation length will reduce to 0 and we arrive at the ground states of fixed-point model, as shown in Fig. 4.8, with the spin-1 projectors in AKLT ground states replaced by identity matrices. Hence, the fixed-point model can be written in terms of spin-$\frac{1}{2}$ operators, due to the enlargement of local Hilbert space into 4 dimensional.
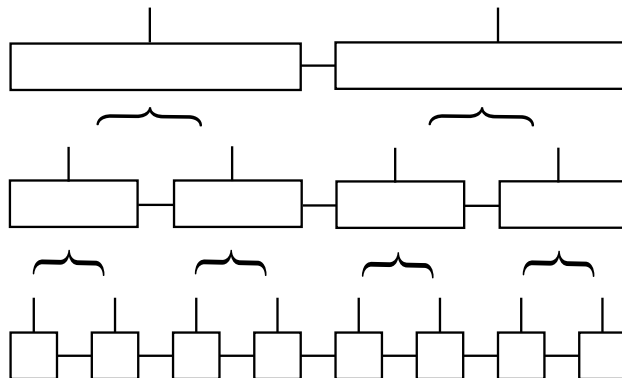
Figure 4.7: Real space renormalisation group transformation for MPS.
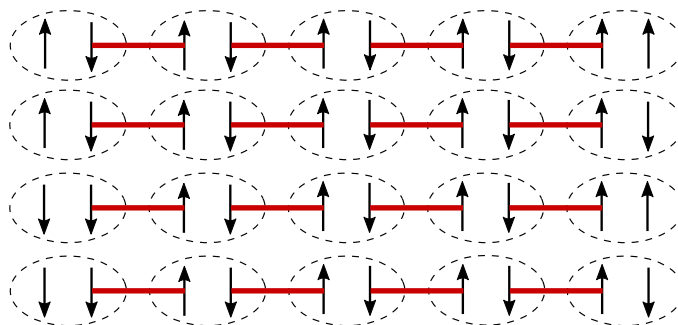
Figure 4.8: Ground states of the fixed-point model.

The Hamiltonian of the fixed-point model is spin-$\frac{1}{2}$ alternating Heisenberg model

$$H_{FP} = \sum_i \sigma_{\mathbf{2i}} \cdot \sigma_{\mathbf{2i+1}}, \tag{4.30}$$

which is exactly solvable (the excitations are the breaking of dimers). The fixed-point model has the same ground state degeneracy and the same symmetries as AKLT model, i.e. in the same SPT phase, albeit the global $SO(3)$ symmetry now acts on two adjacent spin-$\frac{1}{2}$s marked inside the dashed lines in Fig. 4.8.

The edge mode operators become

$$\Psi_L = \sigma_1^z, \Psi_R = \sigma_N^z,$$
$$[H_{FP}, \Psi_L] = [H_{FP}, \Psi_R] = 0. \tag{4.31}$$

The new edge mode operators is strong in the fixed-point model, satisfying our conjecture. The fixed-point model can be related to other models, e.g. XZX cluster model, stack of 4 interacting Majorana chain, etc [57], helping to find more models with Haldane phase.

Chapter 5

Haldane chain

> L'homme est né libre, et partout il
> est dans les fers.
>
> ___
>
> Jean-Jacques Rousseau

We focus on the physical properties of Haldane chain Hamiltonian in Chapter 2, i.e.

$$H_{\text{spin}} = t \sum_i (S_i^+ S_{i+1}^- + \text{h.c.}) + \frac{U}{2} \sum_i (S_i^z)^2 + V \sum_i S_i^z S_{i+1}^z. \qquad (5.1)$$

Ground states of Haldane chain could have the same SPT phase as ground states of AKLT model, and they can also be described faithfully via MPS, despite that the matrices can only be obtained numerically. The symmetries that protect the SPT phase (Haldane phase) are similar to the ones of AKLT model, and the quantum phase transitions can be studied via bosonisation, revealing the physical properties of different phase transitions. More interestingly, we study the phase transitions in the presence of long-range interaction, observing the survival of the Haldane phase and phase transitions with the presence of dipole-dipole interaction.

Historically speaking, Haldane phase is first studied by Duncan Haldane for spin-1 Heisenberg model in 1D, which has the same Haldane phase as Eq. 5.1. It is known that there is gapless excitation in 1D spin-$\frac{1}{2}$ Heisenberg model that can be solved exactly through Bethe ansatz. Haldane then showed that for integer spin, 1D Heisenberg model is gapped using non-linear σ model, while for half integer spin, 1D Heisenberg model is gapless guaranteed by Lieb-Schultz-Mattis theorem [17, 58, 59]. We use a modern

perspective to describe the gapped Haldane phase in terms of SPT phase, and study the phase transitions in the long wavelength limit using bosonisation in this thesis.
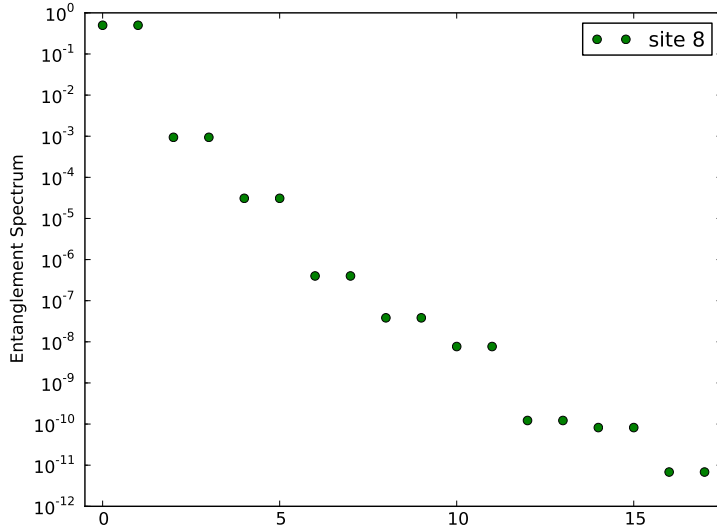
Figure 5.1: Entanglement spectrum of Haldane model in Haldane phase ($U = 6$, $V = 4.5$) with site $L = 16$. Due to the finite size correction, there is a energy gap between $S = 0$ and $S = 1$. The degeneracy in the figure represents the degeneracy of $|\sum S^z| = 1$.

5.1 Phases in Haldane chain ground states

We can easily spot two gapped phases from Haldane chain Hamiltonian Eq. 5.1

- $U \to \infty$, V and t are finite. $H_{eff} = \frac{U}{2} \sum_i (S_i^z)^2$, and we will obtain a unique ferromagnetic ground state $|0000 \cdots 0\rangle$.

- $V \to \infty$, U and t are finite. $H_{eff} = V \sum_i S_i^z S_{i+1}^z$, i.e. antiferromagnetic Ising chain. There are two degenerate antiferromagnetic ground states in OBC depending on the even or odd number of total sites with a bulk $|\cdots + - + - + - \cdots\rangle$.

What Haldane observed in [17, 58] is neither of the two distinct phase. The Haldane phase appears when both U and V are large, as a result of the competition of two phases mentioned.

Haldane chain Hamiltonian has 3 symmetries that can protect the Haldane phase: D_2 symmetry, time-reversal symmetry and bond-centered inversion symmetry, which are proved in Chapter 3.

5.2   Phase transitions in Haldane chain Hamiltonian
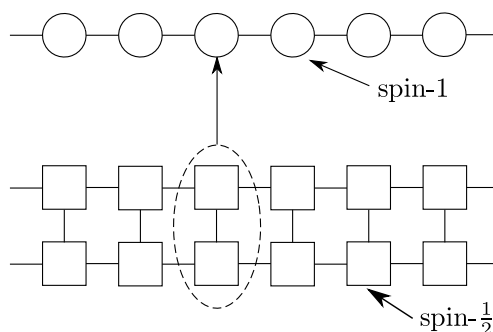
Figure 5.2: Mapping from a spin-1 chain into an effective spin-$\frac{1}{2}$ ladder.

We learn from the previous chapters that the physical system must have particle-hole excitations to perform bosonisation. Hence, the spin-1 Haldane chain cannot be bosonised directly. Due to the fact that spin-$\frac{1}{2}$s can be bosonised after Jordan-Wigner transformation, we can map the spin-1 Haldane chain into an effective model consisting of a spin-$\frac{1}{2}$ ladder [6], as shown in Fig. 5.2. The local Hilbert space has been enlarged from 3 dimensional to 4 dimensional, but it does not affect the results because we are concerning about physics in long wavelength limit, and it can be compared to the previous work based on DMRG [5].

The physical spin operators are mapped as follows

$$
\begin{aligned}
S_i^z &= \sigma_{1,i}^z + \sigma_{2,i}^z, \\
S_i^+ &= \frac{1}{\sqrt{2}}(\sigma_{1,i}^+ + \sigma_{2,i}^+),
\end{aligned}
\tag{5.2}
$$

where 1 and 2 represent the two spin-$\frac{1}{2}$ chains, and S^n and σ^n are spin-1 and spin-$\frac{1}{2}$ operators, respectively.

The Hamiltonian 5.1 (without the staggered transformation) can be rewritten with

spin-$\frac{1}{2}$ operators

$$H = -\frac{t}{2}\sum_i \left[(\sigma_{1,i}^+ + \sigma_{2,i}^+)(\sigma_{1,i+1}^- + \sigma_{2,i+1}^-) + \text{h.c.}\right] + \frac{U}{2}\sum_i (\sigma_{1,i}^z + \sigma_{2,i}^z)^2$$
$$+ V\sum_i (\sigma_{1,i}^z + \sigma_{2,i}^z)(\sigma_{1,i+1}^z + \sigma_{2,i+1}^z),$$
$$= H_t + H_U + H_V. \tag{5.3}$$

Jordan-Wigner transformation for spin-$\frac{1}{2}$ operators is

$$\sigma_{\alpha,j}^z = c_{\alpha,j}^\dagger c_{\alpha,j} - \frac{1}{2},$$
$$\sigma_{\alpha,j}^- = e^{i\pi\sum_{k<j} c_{\alpha,k}^\dagger c_{\alpha,k}} c_{\alpha,j}. \tag{5.4}$$

We study the quantum phase transitions, i.e. phase transitions about the ground states in the physical system, and we know from the analysis above and an analogue of AKLT ground states that total magnetisation for the ground state is zero, i.e. half-filling for the effective spinless fermionised ladder $\langle c_{\alpha,j}^\dagger c_{\alpha,j}\rangle = \frac{1}{2}$. And in bosonic language, lattice spacing is $a \to 0$ in continuous limit and $\rho_{\alpha,0} = \frac{1}{2a}$, $k_F = \frac{\pi}{2a}$ (cf. Eq. A.6 in Appendix A). Thus, we can bosonise the Hamiltonian 5.3 in the following way:

$$c_{\alpha,j} = c_{\alpha,j,L} + c_{\alpha,j,R} \sim \frac{1}{\sqrt{2a}}e^{ik_F x_j}\eta e^{i(\phi_\alpha(x_j)+\theta_\alpha(x_j))} + \frac{1}{\sqrt{2a}}e^{-ik_F x_j}\bar{\eta}e^{i(\phi_\alpha(x_j)-\theta_\alpha(x_j))},$$
$$:c_{\alpha,j}^\dagger c_{\alpha,j}: \sim -\frac{1}{\pi}\partial\phi_\alpha(x_j) + \frac{(-1)^j}{\pi a}\sin(2\phi_\alpha(x_j)),$$
$$\tag{5.5}$$

where η and $\bar{\eta}$ are Majorana operators (explained in Appendix A),

$$\sum_{k<j} :c_{\alpha,k}^\dagger c_{\alpha,k}: \sim \int dx\left[-\frac{1}{\pi}\partial\phi_\alpha(x_j) + \cdots\right] \sim -\frac{1}{\pi}\phi_\alpha(x_j) + \frac{1}{\pi}\phi_\alpha(-\infty), \tag{5.6}$$

where we choose the boundary condition $\phi_\alpha(-\infty) \to 0$ and use the fact that $e^{\sum_{k<j}:c_{\alpha,k}^\dagger c_{\alpha,k}:}$ is Hermitian,

$$e^{\sum_{k<j}:c_{\alpha,k}^\dagger c_{\alpha,k}:} \sim \frac{1}{2}(e^{ik_F x_j}e^{-i\phi_\alpha(x_j)} + e^{-ik_F x_j}e^{i\phi_\alpha(x_j)}). \tag{5.7}$$

With $k_F = \frac{\pi}{2a}$,

$$
\begin{aligned}
\sigma_{\alpha,j}^+ \sigma_{\alpha,j+1}^- + \text{h.c.} &= c_{\alpha,j}^\dagger c_{\alpha,j+1} + \text{h.c.} \\
&\sim \frac{-1}{2\pi a} [e^{i(\phi_\alpha(x_j)+\theta_\alpha(x_j))} e^{-i(\phi_\alpha(x_j+a)+\theta_\alpha(x_j+a))} \\
&\quad + e^{-i(\phi_\alpha(x_j)-\theta_\alpha(x_j))} e^{i(\phi_\alpha(x_j+a)-\theta_\alpha(x_j+a))} + \text{h.c.}] \\
&\quad + \frac{(-1)^j}{2\pi a} [e^{i(\phi_\alpha(x_j)+\theta_\alpha(x_j))} e^{i(\phi_\alpha(x_j+a)-\theta_\alpha(x_j+a))} \\
&\quad + e^{-i(\phi_\alpha(x_j)-\theta_\alpha(x_j))} e^{-i(\phi_\alpha(x_j+a)+\theta_\alpha(x_j+a))} + \text{h.c.}],
\end{aligned}
\tag{5.8}
$$

since we only care about the long wavelength limit (i.e. regime near ground state), we can safely omit the oscillating terms, and

$$
e^{i\phi_\alpha(x+a)} \sim e^{i\phi_\alpha(x)} e^{ia\partial\phi_\alpha(x)} \sim e^{i\phi_\alpha(x)}(1 + ia\partial\phi_\alpha(x) - \frac{a^2}{2}(\partial\phi_\alpha(x))^2 + \cdots),
\tag{5.9}
$$

$$
\begin{aligned}
\sigma_{\alpha,j}^+ \sigma_{\alpha,j+1}^- + \text{h.c.} &\sim \frac{-1}{2\pi a} \left[2 \times \frac{a}{2}((\partial\phi_\alpha(x_j))^2 + (\partial\theta_\alpha(x_j))^2) + 2 \times \frac{a}{2}((\partial\phi_\alpha(x_j))^2 - (\partial\theta_\alpha(x_j))^2) \right] \\
&\sim -\frac{a}{2\pi} \left[(\partial\phi_\alpha(x_j))^2 + (\partial\theta_\alpha(x_j))^2 \right].
\end{aligned}
\tag{5.10}
$$

$$
\begin{aligned}
\sigma_{1,j}^+ \sigma_{2,j+1}^- + \sigma_{2,j}^+ \sigma_{1,j+1}^- + \text{h.c.} &\sim \frac{1}{2\pi a} \left[e^{i(\theta_1(x_j)-\theta_2(x_j+a))} + e^{i(\theta_2(x_j)-\theta_1(x_j+a))} + \text{h.c.} \right] \\
&\sim \frac{2}{\pi a} \cos(\theta_1(x_j) - \theta_2(x_j))
\end{aligned}
\tag{5.11}
$$

Defining $\phi_\pm = \phi_1 \pm \phi_2$ and $\theta_\pm = \frac{1}{2}(\theta_1 \pm \theta_2)$, we get the bosonised form for the first term in Hamiltonian 5.2

$$
\begin{aligned}
H_t &= -\frac{t}{2} \sum_j \left(\sigma_{1,j}^+ \sigma_{1,j+1}^- + \sigma_{2,j}^+ \sigma_{2,j+1}^- + \text{h.c.} \right) + \sum_j \left(\sigma_{1,j}^+ \sigma_{2,j+1}^- + \sigma_{2,j}^+ \sigma_{1,j+1}^- + \text{h.c.} \right) \\
&\sim \frac{t}{2} \int dx \frac{a}{2\pi} \left[(\partial\phi_+)^2 + (\partial\phi_-)^2 \right] + \frac{2a}{\pi} \left[(\partial\theta_+)^2 + (\partial\theta_-)^2 \right] - \frac{2}{\pi a} \cos(2\theta_-).
\end{aligned}
\tag{5.12}
$$

The same bosonisation procedure is exploited for other terms in Hamiltonian,

$$
\begin{aligned}
\sigma_{1,j}^z \sigma_{2,j}^z &= {:}c_{1,j}^\dagger c_{1,j}{::}c_{2,j}^\dagger c_{2,j}{:} \\
&\sim \left[-\frac{1}{\pi}\partial\phi_1(x_j) + \frac{(-1)^j}{\pi a}\sin(2\phi_1(x_j)) \right] \left[-\frac{1}{\pi}\partial\phi_2(x_j) + \frac{(-1)^j}{\pi a}\sin(2\phi_2(x_j)) \right] \\
&\sim \frac{1}{4\pi^2} \left[(\partial\phi_+(x_j))^2 - (\partial\phi_-(x_j))^2 \right] + \frac{1}{2\pi^2 a^2} \left[\cos(2\phi_-(x_j)) - \cos(2\phi_+(x_j)) \right],
\end{aligned}
\tag{5.13}
$$

the final result is given by omitting all the constant and oscillating terms, e.g. terms with $(-1)^j$.

$$
\begin{aligned}
H_U &= \frac{U}{2} \sum_j \left[(\sigma_{1,j}^z)^2 + 2(\sigma_{1,j}^z)(\sigma_{2,j}^z) + (\sigma_{1,j}^z)^2 \right] \\
&= \frac{U}{2} \sum_j \left[2(\sigma_{1,j}^z)(\sigma_{2,j}^z) + \frac{1}{2} \right] \\
&\sim \frac{Ua}{2} \int dx \frac{1}{2\pi^2} \left[(\partial \phi_+(x_j))^2 - (\partial \phi_-(x_j))^2 \right] + \frac{1}{\pi^2 a^2} \left[\cos\left(2\phi_-(x_j)\right) - \cos\left(2\phi_+(x_j)\right) \right].
\end{aligned}
\tag{5.14}
$$

For the nearest-neighbour interaction term, we first look at the intrachain interaction,

$$
\begin{aligned}
:c_{\alpha,j}^\dagger c_{\alpha,j} :: c_{\alpha,j+1}^\dagger c_{\alpha,j+1} :\sim\ & [\psi_R^\dagger(x_j)\psi_R(x_j)\psi_R^\dagger(x_j+a)\psi_R(x_j+a) \\
& + \psi_R^\dagger(x_j)\psi_R(x_j)\psi_L^\dagger(x_j+a)\psi_L(x_j+a) + \psi_L^\dagger(x_j)\psi_L(x_j)\psi_R^\dagger(x_j+a)\psi_R(x_j+a) \\
& + \psi_L^\dagger(x_j)\psi_L(x_j)\psi_L^\dagger(x_j+a)\psi_L(x_j+a)] - [\psi_R^\dagger(x_j)\psi_L(x_j)\psi_L^\dagger(x_j+a)\psi_R(x_j+a) \\
& + \psi_L^\dagger(x_j)\psi_R(x_j)\psi_R^\dagger(x_j+a)\psi_L(x_j+a) + \psi_R^\dagger(x_j)\psi_L(x_j)\psi_R^\dagger(x_j+a)\psi_L(x_j+a) \\
& + \psi_L^\dagger(x_j)\psi_R(x_j)\psi_L^\dagger(x_j+a)\psi_R(x_j+a)] \\
\sim\ & \frac{1}{\pi^2}(\partial \phi_\alpha(x_j))^2 - \frac{1}{4\pi^2 a^2}(e^{i(-2\phi_\alpha(x_j)+2\phi_\alpha(x_j))} + \text{h.c.}) \\
& + \frac{1}{4\pi^2 a^2}(e^{i(2\phi_\alpha(x_j)+2\phi_\alpha(x_j))} + \text{h.c.}) \\
\sim\ & \frac{1}{\pi^2}(\partial \phi_\alpha(x_j))^2 - \frac{1}{4\pi^2 a^2}(e^{-i\partial\phi_\alpha(x_j)} + \text{h.c.}) + \frac{1}{2\pi^2 a^2}\cos\left(4\phi_\alpha(x_j)\right) \\
\sim\ & \frac{2}{\pi^2}(\partial \phi_\alpha(x_j))^2 + \frac{1}{2\pi^2 a^2}\cos\left(4\phi_\alpha(x_j)\right).
\end{aligned}
\tag{5.15}
$$

$$
\begin{aligned}
V \sum_{\alpha,j} \sigma_{\alpha,j}^z \sigma_{\alpha,j+1}^z &= \frac{U}{2} \sum_{\alpha,j} :c_{\alpha,j}^\dagger c_{\alpha,j} :: c_{\alpha,j+1}^\dagger c_{\alpha,j+1} : \\
&\sim Va \int dx \frac{2}{\pi^2} \left[(\partial \phi_1)^2 + (\partial \phi_2)^2 \right] + \frac{1}{2\pi^2 a^2} \left[\cos\left(4\phi_1\right) + \cos\left(4\phi_2\right) \right] \\
&\sim Va \int dx \frac{1}{\pi^2} \left[(\partial \phi_+)^2 + (\partial \phi_-)^2 \right] + \frac{1}{\pi^2 a^2} \cos\left(2\phi_+\right)\cos\left(2\phi_-\right).
\end{aligned}
\tag{5.16}
$$

Similar to Eq. 5.13, the intrachain interaction becomes

$$V \sum_j \sigma^z_{1,j}\sigma^z_{2,j+1} + \sigma^z_{2,j}\sigma^z_{1,j+1} = V \sum_j :c^\dagger_{1,j}c_{1,j}::c^\dagger_{2,j+1}c_{2,j+1}: + :c^\dagger_{2,j}c_{2,j}::c^\dagger_{1,j+1}c_{1,j+1}:$$

$$\sim Va \int dx \frac{1}{2\pi^2} \left[(\partial\phi_+)^2 - (\partial\phi_-)^2\right] +$$

$$\frac{1}{\pi^2 a^2} \left[\cos(2\phi_+) - \cos(2\phi_-)\right]. \tag{5.17}$$

Combining all the interaction terms, we obtain

$$H_V = V \sum_{\alpha,\beta,j} \sigma^z_{\alpha,j}\sigma^z_{\beta,j+1}$$

$$\sim Va \int dx \frac{1}{\pi^2} \left[\frac{3}{2}(\partial\phi_+)^2 + \frac{1}{2}(\partial\phi_-)^2\right] + \frac{1}{\pi^2 a^2}\cos(2\phi_+)\cos(2\phi_-) \tag{5.18}$$

$$+ \frac{1}{\pi^2 a^2}\left[\cos(2\phi_+(x_j)) - \cos(2\phi_-(x_j))\right].$$

We can combine all three terms in the Hamiltonian, and reorder them in terms of $+$ and $-$ sectors.

$$H = H_+ + H_- + H_{+-}, \tag{5.19}$$

$$H_+ = \int dx \left(\frac{Ua}{4\pi^2} + \frac{3V}{2\pi^2} + \frac{ta}{4\pi}\right)(\partial\phi_+)^2 + \frac{ta}{\pi}(\partial\theta_+)^2 + \frac{2Va - Ua}{\pi^2 a^2}\cos(2\phi_+)$$

$$= \frac{u_+}{2\pi} \int dx \left[K_+(\partial\theta_+)^2 + \frac{1}{K_+}(\partial\phi_+)^2\right] + \int dx \frac{g_1}{(\pi a)^2}\cos(2\phi_+), \tag{5.20}$$

$$H_- = \int dx \left(-\frac{Ua}{4\pi^2} + \frac{V}{2\pi^2} + \frac{ta}{4\pi}\right)(\partial\phi_-)^2 + \frac{ta}{\pi}(\partial\theta_-)^2 + \frac{Ua - 2Va}{\pi^2 a^2}\cos(2\phi_-) - \frac{t}{\pi a}\cos(2\theta_-)$$

$$= \frac{u_-}{2\pi} \int dx \left[K_-(\partial\theta_-)^2 + \frac{1}{K_-}(\partial\phi_-)^2\right] + \int dx \left[\frac{g_2}{(\pi a)^2}\cos(2\phi_-) + \frac{g_3}{(\pi a)^2}\cos(2\theta_-)\right], \tag{5.21}$$

$$H_{+-} = \int dx \frac{Va}{2\pi^2}\cos(2\phi_+)\cos(2\phi_-) = \int dx \frac{g_4}{(\pi a)^2}\cos(2\phi_+)\cos(2\phi_-). \tag{5.22}$$

We can obtain the renormalised velocity, Luttinger coefficients and coupling coefficients from Eq. 5.20, 5.21, 5.22,

$$u_+ = ta\sqrt{1 + \frac{U + 6V}{\pi t}}, K_+ = \frac{2}{\sqrt{1 + \frac{U+6V}{\pi t}}}, g_1 = \frac{(2V - U)a}{2} = -g_2,$$

$$u_- = ta\sqrt{1 + \frac{2V - U}{\pi t}}, K_- = \frac{2}{\sqrt{1 + \frac{2V-U}{\pi t}}}, g_3 = -\pi ta, g_4 = Va. \tag{5.23}$$

Since we have obtained the bosonised Hamiltonian 5.19, we can study the phase transition via analysing the relevance of sine-Gordon Hamiltonian in the renormalisation group flow. For example, we study the relevance of the g_1 term in Eq. 5.20. The correlation function (Eq. A.8 in Appendix A) can be written as

$$
\begin{aligned}
\langle \cos\left(2\phi(r_1)\right) \cos\left(2\phi(r_2)\right) \rangle &\propto \langle e^{2i\phi_+(r_1)} e^{-2i\phi_+(r_2)} \rangle \\
&\propto e^{-2K_+ F_1(r_1-r_2)} \sim (r_1 - r_2)^{-2K_+},
\end{aligned}
\tag{5.24}
$$

then we can obtain the growth of g_1 term in the Hamiltonian 5.20 in the long wavelength limit

$$
\frac{g_1}{(\pi a)^2} \int dx\, d\tau \cos\left(2\phi_+\right) \sim \frac{g_1}{(\pi a)^2} l^{2-K_+},
\tag{5.25}
$$

where $l = |r_1 - r_2|$. Thus, if $K_+ > 2$, the cosine term vanishes to 0 as $l \to \infty$ (i.e. long wavelength limit), which means the g_1 term is irrelevant and the Hamiltonian can be treated as a Luttinger liquid (i.e. gapless). If $K_+ < 2$, the g_1 term goes to infinity as $L \to \infty$, which means the g_1 term is relevant at long wavelength limit, resulting in a gapped phase.

Similar argument can be used for Eq. 5.21. It is easy to verify that g_2 term is relevant when $K_- < 2$, and g_3 term is relevant when $K_- > \frac{1}{2}$.

The first observation would be g_1 term is always relevant, since

$$
K_+ = \frac{2}{\sqrt{1 + \frac{U+6V}{\pi t}}} < 2, \forall t, U, V > 0.
\tag{5.26}
$$

But if g_1 changes sign, ϕ_+ will localise at different values, leading to a phase transition. $g_1 < 0$, i.e. $U > 2V$, corresponds to the unique ferromagnetic ground state $|000\cdots\rangle$. Moreover, the system is always gapped, because with $K_- < 2$, g_2 term is always relevant too. For the case of $g_1 > 0$, the system can be in the Haldane phase or the antiferromagnetic phase, depending on H_- sector. Still we can identify $U = 2V$ as the phase transition line between ferromagnetic and Haldane phase. Note that the phase transition line obtained by bosonisation is not exactly the same as the one from numerical simulation or experiments, because we omit the higher order terms, which in general could change the position where phase transition happens.

For the transition between Haldane and antiferromagnetic phases, we have $g_1 > 0$, which determines the sign of g_2. In both of the phases, we have $g_2 < 0$, $g_3 < 0$. The two phases are distinguished by g_2 or g_3 term is more relevant than the other. In Haldane

phase, g_2 term is more relevant, while g_3 term is more relevant in antiferromagnetic phase. Thus the phase transition occurs at $K_- = 1$:

- $K_- < 1$, g_2 term is more relevant than g_3 term. The system is in Haldane phase.

- $K_- > 1$, g_3 term is more relevant than g_2 term. The system is in antiferromagnetic phase.

More remarkably, the phase transition that occurs at $K_- = 1$ has Ising universality class. This can be seen by the equivalence between H_- at $K_- = 1$, $g_2 = g_3$ and massless Majorana fermion field theory at critical point between topologically non-trivial phase and trivial phase.

These two phase transitions can be understood using CFT [25, 57]. The phase transition between ferromagnetic and Haldane phases happens when $g_1 = 0$, resulting in a gapless Luttinger liquid

$$H_+ = \frac{u_+}{2\pi} \int dx \left[K_+ (\partial \theta_+)^2 + \frac{1}{K_+} (\partial \phi_+)^2 \right]. \tag{5.27}$$

Hence the phase transition between ferromagnetic and Haldane phases can be described asymptotically as a bosonic CFT with central charge $c = 1$ (equivalent to a free Luttinger liquid).

As for the phase transition between Haldane and antiferromagnetic phases, we first generalise this phase transition as a transition between Haldane phase and a $\mathbb{Z}_2$ symmetry breaking phase. Since cluster model ($H = \sum_n \sigma_n^x \sigma_n^z \sigma_{n+1}^x$) is in Haldane phase [57], the phase transition is equivalent to the one between cluster model and Ising chain with transverse magnetic field. If we operate Jordan-Wigner transformation to both cluster model and Ising chain with transverse magnetic field, we will end up with 2-chain (i.e. 2 decoupled Kitaev chain stacking together) and Kitaev chain. The phase transition between 2-chain and Kitaev chain has been studied, and it can be described as an Ising CFT with central charge $c = \frac{1}{2}$ [57], consistent with the prediction of Ising universality class from bosonisation mentioned above.

We can also discuss the consequence of having coupled term H_{+-} (g_4 term). When the system is in the ferromagnetic or antiferromagnetic phase, g_3 term is more relevant than g_2 term, and g_4 term can be ignored in the analysis. While in Haldane phase, g_2 term is more relevant than g_3 term, with $g_2 < 0$. Therefore, $\cos(2\phi_-)$ localises at 1, g_4

term becomes $H_{+-} = \int dx \frac{g_4}{\pi^2 a^2} \cos{(2\phi_+)}$. In this situation, both g_1 and g_4 are larger than 0, leading to the same value (-1) where $\cos{(2\phi_+)}$ localises, which does not lead to any inconsistency. Therefore, g_4 term does not affect the phases mentioned above.

5.3   The impact of long-range interaction
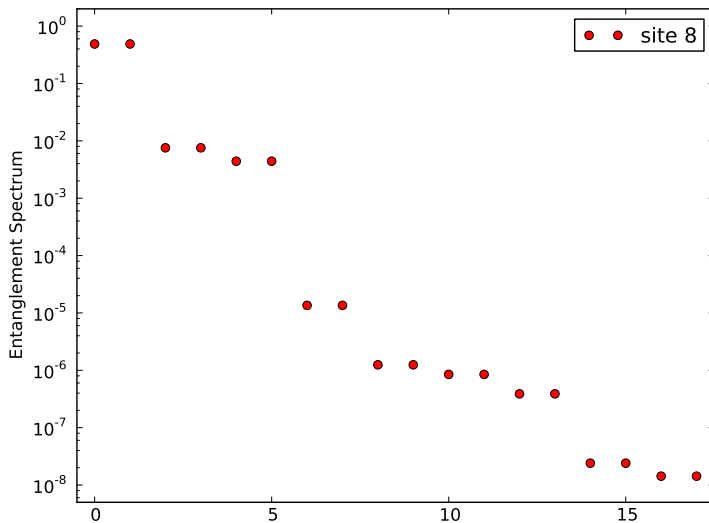
Figure 5.3: Entanglement spectrum of Haldane model with next-nearest-neighbour inter-action with site $L = 16$. The system is in Haldane phase without next-nearest-neighbour interaction (Fig. 5.1), and apparently, Haldane phase survives with presence of next-nearest-neighbour interaction.

Using bosonisation, we can study the phase transition for the system with long-range interaction in asymptotically long wavelength limit. The Hamiltonian now is included with the long-range interaction term:

$$H = t \sum_i (S_i^+ S_{i+1}^- + \text{h.c.}) + \frac{U}{2} \sum_i (S_i^z)^2 + \sum_{i,r>0} \frac{V}{r^3} S_i^z S_{i+r}^z. \tag{5.28}$$

Here we include the entire dipole-dipole interaction in the Hamiltonian. This is moti-vated from the ultracold atom experiments, whose interaction usually does not confine to the nearest neighbour or next nearest neighbour. Especially in some state-of-the-art

experiments [3], long-range dipole-dipole interaction is present, which could in principle differ from the phases and phase transitions with only nearest-neighbour interaction.

The bosonised interaction term becomes

$$
\begin{aligned}
\frac{V}{r^3} S_j^z S_{j+r}^z &= \frac{V}{r^3}(\sigma_{1,j}^z + \sigma_{2,j}^z)(\sigma_{1,j+r}^z + \sigma_{2,j+r}^z) \\
&= \frac{V}{r^3}\left[\sum_\alpha \left(\sigma_{\alpha,j}^z \sigma_{\alpha,j+r}^z\right) + \sigma_{1,j}^z \sigma_{2,j+r}^z + \sigma_{2,j}^z \sigma_{1,j+r}^z\right].
\end{aligned}
\tag{5.29}
$$

$$
\begin{aligned}
\frac{V}{r^3}\left[\sum_\alpha (\sigma_{\alpha,j}^z \sigma_{\alpha,j+r}^z)\right] &\sim \frac{V}{r^3}[\sum_\alpha \frac{1}{\pi^2}(\partial\phi_\alpha(x_j)) + \frac{(-1)^r}{4\pi^2 a^2}(e^{2ira\partial\phi_\alpha(x_j)} + \text{h.c.}) \\
&+ \frac{(-1)^{r-1}}{4\pi^2 a^2}(e^{4i\phi_\alpha(x_j)} + \text{h.c.})] \\
&\sim \frac{V}{2\pi^2 r^3}[(\partial\phi_+(x_j))^2 + (\partial\phi_-(x_j))^2] + \frac{V(-1)^{r-1}}{\pi^2 r}[(\partial\phi_+(x_j))^2 \\
&+ (\partial\phi_-(x_j))^2] + \frac{V(-1)^{r-1}}{\pi^2 a^2 r^3}\cos(2\phi_+(x_j))\cos(2\phi_-(x_j)).
\end{aligned}
\tag{5.30}
$$

$$
\begin{aligned}
\frac{V}{r^3}\left(\sigma_{1,j}^z \sigma_{2,j+r}^z + \sigma_{2,j}^z \sigma_{1,j+r}^z\right) &\sim \frac{2}{\pi^2 a^2}(\partial\phi_1(x_j))(\partial\phi_2(x_j)) \\
&+ \frac{(-1)^{r-1}}{\pi^2 a^2}\left[\cos(2\phi_+(x_j)) - \cos(2\phi_-(x_j))\right]
\end{aligned}
\tag{5.31}
$$

$$
\begin{aligned}
\widetilde{H}_V &= \sum_{r=1}^\infty \frac{V}{r^3}\sum_j S_i^z S_{i+r}^z \\
&\sim \sum_{r=1}^\infty \frac{1}{r^3}\frac{Va}{2\pi^2}[(\partial\phi_+(x_j))^2 + (\partial\phi_-(x_j))^2] + \sum_{r=1}^\infty \frac{(-1)^{r-1}}{r}\frac{Va}{2\pi^2}[(\partial\phi_+(x_j))^2 + (\partial\phi_-(x_j))^2] \\
&+ \sum_{r=1}^\infty \frac{1}{r^3}\frac{Va}{2\pi^2}[(\partial\phi_+(x_j))^2 - (\partial\phi_-(x_j))^2] + \sum_{r=1}^\infty \frac{(-1)^{r-1}}{r^3}\frac{1}{\pi^2 a^2}\left[\cos(2\phi_+) - \cos(2\phi_-)\right] \\
&\sim \frac{Va}{2\pi^2}\int dx(2\zeta(3) + \log 2)(\partial\phi_+)^2 + (\log 2)(\partial\phi_-)^2 \\
&+ \frac{V}{\pi^2 a}\frac{3}{4}\zeta(3)\left[\cos(2\phi_+)\cos(2\phi_-) + \cos(2\phi_+) - \cos(2\phi_-)\right],
\end{aligned}
\tag{5.32}
$$

where Riemann zeta function $\zeta(n) = \sum_{a=1}^\infty \frac{1}{a^n}$, $\sum_{a=1}^\infty \frac{(-1)^{a-1}}{a} = \log 2$, $\sum_{a=1}^\infty \frac{(-1)^{a-1}}{a^3} = \frac{3}{4}\zeta(3)$.

5. HALDANE CHAIN

We can obtain the Hamiltonian in the $+$ and $-$ sectors with the presence of long-range dipole-dipole interaction:

$$H = \widetilde{H}_+ + \widetilde{H}_- + \widetilde{H}_{+-}, \tag{5.33}$$

$$\widetilde{H}_+ = \frac{\widetilde{u}_+}{2\pi} \int dx \left[\widetilde{K}_+ (\partial \theta_+)^2 + \frac{1}{\widetilde{K}_+} (\partial \phi_+)^2 \right] + \int dx \frac{\widetilde{g}_1}{(\pi a)^2} \cos(2\phi_+),$$

$$\widetilde{H}_- = \frac{\widetilde{u}_-}{2\pi} \int dx \left[\widetilde{K}_- (\partial \theta_-)^2 + \frac{1}{\widetilde{K}_-} (\partial \phi_-)^2 \right] + \int dx \frac{\widetilde{g}_2}{(\pi a)^2} \cos(2\phi_-) \frac{\widetilde{g}_3}{(\pi a)^2} \cos(2\theta_-),$$

$$\widetilde{H}_{+-} = \frac{\widetilde{g}_4}{(\pi a)^2} \cos(2\phi_-) \cos(2\theta_-).$$

$$\tag{5.34}$$

$$\widetilde{u}_+ = ta\sqrt{1 + \frac{U + 2AV}{\pi t}}, \widetilde{K}_+ = \frac{2}{\sqrt{1 + \frac{U+2AV}{\pi t}}}, \widetilde{g}_1 = \frac{2CV - U}{2} = -\widetilde{g}_2,$$

$$\widetilde{u}_- = ta\sqrt{1 + \frac{2BV - U}{\pi t}}, \widetilde{K}_- = \frac{2}{\sqrt{1 + \frac{2BV-U}{\pi t}}}, \widetilde{g}_3 = g_3 = -t\pi a, \widetilde{g}_4 = CVa,$$

$$\tag{5.35}$$

where $A = \zeta(3) + \log 2$, $B = \log 2$, $C = \frac{3}{4}\zeta(3)$.

There exists a difference from the bosonisation calculation with or without long-range interaction, which is the existence of terms like $\frac{V}{n^3} \partial\phi_\alpha(x) \partial\phi_\alpha(x + na)$. For the case without long-range interaction, we can safely Taylor expand the term and omit the higher order derivatives, because they are less relevant. When $n \to \infty$ (within thermodynamic limit), $\partial\phi(x)$ is continuous and $\frac{1}{n^3} \to 0$, we can write the term as $\frac{V}{n^3} \partial\phi_\alpha(x) \partial\phi_\alpha(x)$, which does not change the result within renormalisation group theory.

The analysis for phase transitions is the same as before, but with new Luttinger and coupling coefficients. Phase transition between ferromagnetic and Haldane phases occurs when $\widetilde{g}_1 = 0$, i.e. $U = 2CV$. In addition, phase transition between Haldane and antiferromagnetic phases occurs when $\widetilde{K}_- = 1$, which infers the existence of Ising universality class with or without long-range interaction.

Another intriguing question is under what condition our bosonisation approach is not valid due to the long-range interaction. As we can see, when the exponent of

long-range interaction $\left(\frac{V}{r^\gamma}\right)$ $\gamma < 2$,

$$\sum_{r=1}^{\infty} \frac{(-1)^{r-1}}{r^\gamma} \to \infty, \tag{5.36}$$

coefficients A and B in Eq. 5.35 diverge, implying that bosonisation is no longer applicable (in fact, $\gamma = 2$ will lead to inconsistency in the summation as well). The assumption of bosonisation that there are low-energy sound modes is not true anymore. Thus, our analytic approach cannot determine whether the Haldane phase could survive with the presence of a long-range interaction of exponent $\gamma \leq 2$.

This conclusion is equivalent to the fact that a physical system with a long-range dipole-dipole interaction ($\gamma = 3$) has the same phases as a physical system with interaction cutoffs (e.g. system with nearest-neighbour interaction or next-nearest-neighbour interaction). Moreover, there have been other studies about the impact of long-range interaction in low-dimensional systems [60, 61, 62, 63], and the result that long-range dipole-dipole interaction will not jeopardise the Haldane phase have been obtained via different methods, consistent with our result.

Chapter 6

Extended Bose Hubbard model

> All in all, it's just another brick in the wall.
>
> ———————————————————
>
> Pink Floyd

In previous chapters, we analyse two spin-1 models that have Haldane phase, i.e. AKLT model, and Haldane chain model. The virtue of studying the models is that the models have many symmetries that protect Haldane phase (SPT phase), and analytical methods are used to study the edge modes in AKLT model and long range interaction's impact on Haldane chain. As observed in Chapter 2, 1D extended Bose Hubbard model (EBHM) can be derived directly from dipolar atoms in 1D optical lattice, having closer relation to the state-of-the-art experiment setups. We analyse many properties of EBHM by comparing to the known results for AKLT and Haldane chain models in this chapter.

6.1 SPT phase in EBHM

Since we have examined the symmetries that protect SPT phases in spin-1 language. We can map the EBHM Hamiltonian (Eq. 6.1) into the spin-1 counterpart (Eq. 6.2).

$$H = -t \sum_i (a_i^\dagger a_{i+1} + \text{h.c.}) + \frac{U}{2} \sum_i n_i(n_i - 1) + V \sum_i n_i n_{i+1}. \qquad (6.1)$$

$$H_{\text{spin}} = -t \sum_i (S_i^+ S_{i+1}^- + \text{h.c.}) + \frac{U}{2} \sum_i (S_i^z)^2 + V \sum_i S_i^z S_{i+1}^z + \Delta H, \qquad (6.2)$$

$$\Delta H = -t\xi \sum_i [S_i^z S_{i+1}^+ S_{i+1}^- + S_i^- S_i^z S_{i+1}^+ + S_i^- S_{i+1}^z S_{i+1}^+ +$$
$$S_i^+ S_{i+1}^- S_{i+1}^z + \xi(S_i^z S_i^+ S_{i+1}^- S_{i+1}^z + S_i^+ S_i^z S_{i+1}^z S_{i+1}^-)], \tag{6.3}$$

The mapped spin-1 Hamiltonian without ΔH term is identical to spin-1 Haldane chain Hamiltonian (Eq. 5.1). But ΔH term breaks many symmetries that Haldane chain model have and protect Haldane phase.

- Time reversal symmetry: $T = \prod_j e^{i\pi S_j^y} K$, which changes the spin operators as $S^{x,y,z} \to -S^{x,y,z}$. Hence, $T\Delta HT \neq \Delta H$, $TH_{\text{spin}}T \neq H_{\text{spin}}$, time reversal symmetry is explicitly broken in Hamiltonian 6.2.

- D_2 symmetry: $R_x = \prod_j e^{i\pi S_j^x}$, $R_z = \prod_j e^{i\pi S_j^z}$, which changes the spin operators as $S^{x,z} \to -S^{x,z}$. Hence, $R_x\Delta HR_x \neq \Delta H$, $R_z\Delta HR_z \neq \Delta H$, $R_xH_{\text{spin}}R_x \neq H_{\text{spin}}$, $R_zH_{\text{spin}}R_z \neq H_{\text{spin}}$, D_2 symmetry is explicitly broken in Hamiltonian 6.2.

- Inversion symmetry: (bond-centered) inversion symmetry cannot be written into local terms, but it is obvious to find out that the bosonic Hamiltonian 6.1 preserve inversion symmetry. Since the inversion symmetry is the same both in bosonic or spin language, H_{spin} preserve the inversion symmetry.

Beware that the time reversal symmetry in spin language is not the same as the time reversal symmetry in bosonic language, which EBHM has but does not protect the Haldane phase. Summarising, the Haldane phase in EBHM can only be protected by bond-centered inversion symmetry.

From Fig. 6.1, we can clearly verify that bond-centered inversion symmetry protects the degeneracy in Haldane phase. Moreover, compared to AKLT or Haldane chain models, Haldane phase in EBHM is only protected by bond-centered inversion symmetry, which relies on the geometry of the chain (e.g. even or odd sites of the chain), which is much more fragile.

6.1.1 Absence of edge mode in EBHM

A big difference between 1D EBHM and its spin-1 counterparts (AKLT and Haldane chain models) is the absence of edge mode in EBHM. If there exists any edge mode acting on one edge in EBHM Ψ, and the edge mode Ψ can change one ground state
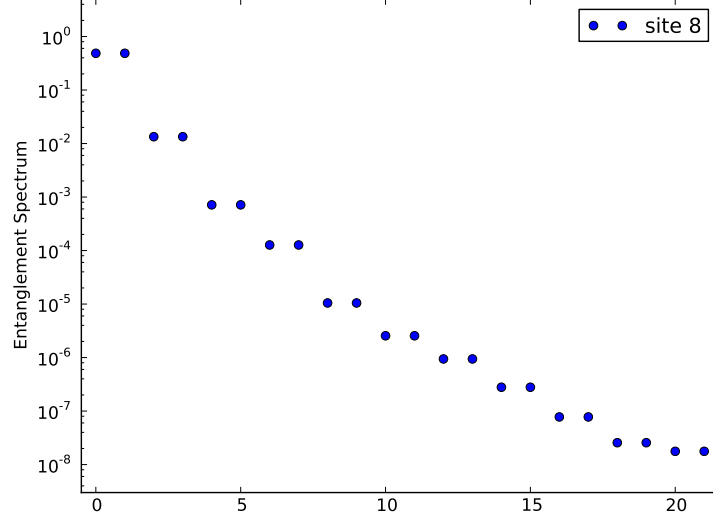
(a) Entanglement spectrum of 1D EBHM in Haldane phase ($U = 6$, $V = 4.5$) of size $L = 16$ with subsystem cut at site 8. The system has bond-centered inversion symmetry.
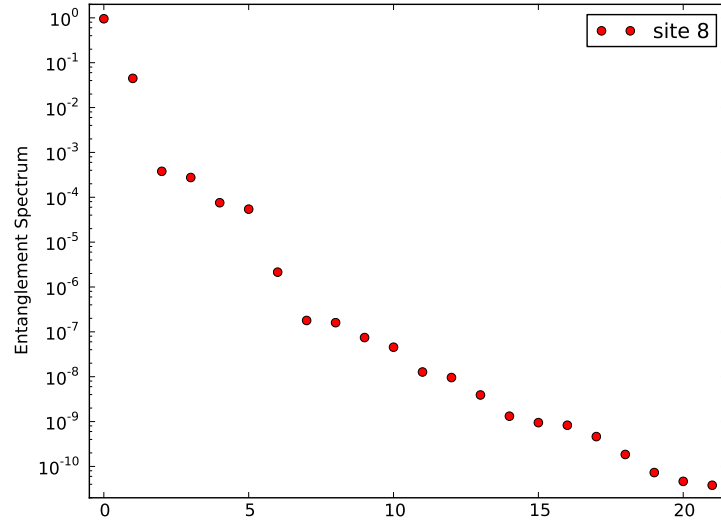
(b) Entanglement spectrum of 1D EBHM in Haldane phase ($U = 6$, $V = 4.5$) of size $L = 16$ with subsystem cut at site 8. The system has inversion symmetry but not bond-centered.

Figure 6.1: Entanglement spectra of 1D EBHM with bond-centered inversion symmetry preserved or broken.

to another, i.e. $\Psi |\text{GS1}\rangle = |\text{GS2}\rangle$. Therefore, the two ground states break the bond-centered inversion symmetry that is essential to protect the SPT phase in EBHM, contradicting from the fact that ground state degeneracy arises from bond-centered inversion symmetry of the ground states. Thus edge modes are absent in EBHM.

Since we construct explicitly the edge mode for spin-1 Haldane phase, the ground states of AKLT or Haldane chain models break the (bond-centered) inversion symmetry. But because there are more symmetries that can protect Haldane phase, the ground state degeneracy will survive despite of the inversion symmetry breaking. It is also easy to see that for any global symmetry that can be written in local terms, e.g. time reversal symmetry, $SO(3)$ symmetry, etc, it is compatible with the edge modes, cf. Fig. 3.6.

6.2   Phase diagram of EBHM

The phase diagram of EBHM is richer than the one of Haldane chain model, because the later model is an approximation only when U is large, i.e. a truncation of Hilbert space is reasonable. Firstly, we assume that the truncation of Hilbert space is a good approximation, then we could identify 3 phases, similar to the case of Haldane chain:

- $U \to \infty$, V and t are finite. $H_{eff} = \frac{U}{2} \sum_j (n_j)^2$, and at average filling $\bar{n} = 1$, we obtain a Mott insulating phase, which is the ferromagnetic phase with unique ground state in Haldane chain.

- $V \to \infty$, U and t are finite. $H_{eff} = V \sum_j n_j n_{j+1}$, and at average filling $\bar{n} = 1$, we obtain a density wave (DW) phase, which is the antiferromagnetic phase in Haldane chain.

- There also exists a Haldane phase in between Mott and DW phases, analogous to the Haldane phase in Haldane chain model.

The Haldane phase cannot be characterised via local order parameter, but a non-local string order parameter does not vanish to 0,

$$\mathcal{O}(|j - k|) = \delta n_j \exp\left(i\pi \sum_{j < m < k} \delta n_m\right) \delta n_k, \ \ \delta n_j = n_j - \bar{n}. \tag{6.4}$$

The order parameter is the same as the string order parameter for Haldane phase in spin-1 language after Holstein-Primarkoff transformation, indicating the same SPT phase in EBHM.

Another phase can be easily spotted, i.e. superfluid phase when $t \to \infty$. A sketch of the phase diagram is shown in Fig. 6.2.

Figure 6.2: A sketch of EBHM's phase diagram. The figure is taken from [6] with permission.

There is one more phase that cannot be captured by the analysis based on the truncation of Hilbert space, i.e. supersolid phase when t and V are large and U is relatively small. This can be understood naively by considering large V should induce local checkerboard structure while large t brings superfluidity in the system, and supersolid phase can be seen as a combination of superfluidity and locally ordered phase. More detailed analysis is in [64], and we focus on the 3 gapped phases (Mott, Haldane and DW phases) within this thesis.

6.3 Connection to ultracold atom experiments

It is significant that the Haldane phase can be observed in ultracold atom experiments, which could allow us to verify the theories on 1D SPT phases. According to the prediction in Chapter 5 that the presence of long-range dipole-dipole interaction ($\propto \frac{1}{r^3}$)

does not destroy the Haldane phase, we expect that the Haldane phase in 1D EBHM will also survive in an experiment with long-range dipole-dipole interaction.

With the new development of quantum gas microscopy [65, 66], which can visualise single atom in optical lattices, one can observe different phases of 1D EBHM.
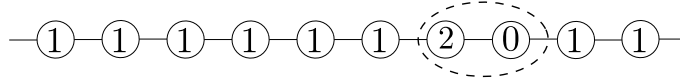
(a) Mott insulating phase of EBHM. The dashed line illustrates the possible low-energy excitations in ultracold atom experiments.
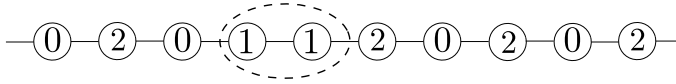
(b) Density wave phase of EBHM. The dashed line illustrates the possible low-energy excitations in ultracold atom experiments.
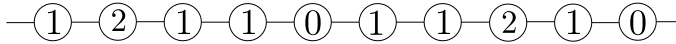
(c) Haldane phase of EBHM. The absence of local order can be seen in this figure.

Figure 6.3: An illustration of different phases of EBHM in quantum gas microscopy experiment.

It is worth mentioning that it is possible to measure the string order parameter 6.4 from a state-of-the-art experiment [67], which makes it possible to identify the Haldane phase in an experiment with dipolar atoms trapped in 1D optical lattice, leading to the possible confirmation of our bosonisation prediction that long-range dipole-dipole interaction will not jeopardise the Haldane phase.

Chapter 7

Conclusions

7.1 Overview

In this thesis we presented a comprehensive analysis of SPT phases in 1D systems, with emphases on edge modes and systems with long-range interaction. Firstly, we derived the theoretical models from a realistic experimental setup, tracing back the motivations to study EBHM and its spin-1 counterparts, i.e. Haldane chain and AKLT models. The analytic and numerical methods that have been used extensively later are introduced too, leading to a thorough understanding of the mechanism of symmetry protected nature of SPT phase and phenomena such as symmetry fractionalisation.

Secondly, we concentrated on a spin-1 toy model, i.e. AKLT model, which has the advantage of using analytic approaches. The ground states of AKLT model are constructed exactly via MPS description, and we constructed a parent Hamiltonian through the properties of the ground states. This method not only can be used for this specific case, but also for other strongly correlated systems. The gapped and symmetry protected properties of ground states can be easily observed in this model, and from those properties we constructed the edge mode operators. We also summarised the previous work on edge modes in 1D systems, motivating future research in this direction. Another interesting result would be exploiting real space renormalisation group method to AKLT model, which can be demonstrated explicitly, leading to a fixed-point model with strong edge modes.

Thirdly, we studied the celebrated spin-1 Haldane chain model, moving closer to possible ultracold atom experiment setups. Three gapped phases are identified, and

a natural question is solved in the context: how the phase transitions between these phases behave. Instead of provoking the extensive numerical simulation on this, we used bosonisation to analyse the asymptotically long wavelength limit of the Haldane chain ground states. Our result reveals the phase transitions' universality class and possible CFT descriptions. In addition, we added the long-range interaction to the system, and obtained the result that long-range dipole-dipole interaction will not jeopardise the Haldane phase, while bosonisation cannot deal with longer-range interaction.

Eventually, we moved on to 1D EBHM, which could be realised in state-of-the-art experiments. We found out that 1D EBHM can have more phases compared to Haldane chain, due to the fact that it can be mapped into spin-1 models under the assumption of the truncation of local Hilbert space. We focused on the regime when this assumption works, finding the correspondence between the phases in EBHM and the ones in Haldane chain. A possible confirmation for the Haldane phase via dipolar bosonic gases in 1D optical lattices are proposed using quantum gas microscopy methods.

7.2   Overlook

Despite that the classification of 1D SPT phases has been thoroughly studied, there are still many aspects that we do not understand well. For instance, the research about edge modes in 1D systems is not well understood, especially under what condition there could exist strong edge modes, leading to some useful applications for quantum computation in finite temperature. From our example of AKLT model, a more general and complete understanding is expected, possibly by analysing the properties of the exactly solvable models that have strong edge modes. It is also important to expect an experimental realisation of such systems, leading to the construction of more practical models for ultracold atom experiments.

There is another significant area of research that needs to be understood, i.e. the phase transitions between SPT phases (and trivial phases). It is not obvious to connect our knowledge on symmetry breaking phase transitions with the phase transitions between SPT phases. As we have demonstrated in this thesis, an Ising universality class/Ising CFT is expected between the Haldane phase and DW phase in 1D EBHM. Since it is possible to perform experiments with dipolar bosonic gases in optical lattices, one can also think of possible experimental methods to confirm the critical theories.

Moreover, there are more complicated cases if we consider anyonic systems, which broadens our understanding on quantum phase transitions in general.

As we can see, it is natural to have long-range interactions in ultracold atom experiments, while it is more difficult to obtain the theoretical results on systems with long-range interaction. It has been an interest for physicists to consider the effect of long-range interaction in many different systems, and now there is one open question, i.e. how long-range interaction renders systems with topological or SPT phases. We studied a specific phase (Haldane phase) with the presence of long-range interaction, and more general arguments about systems in higher dimensions are still yet to come.

7. CONCLUSIONS

Appendix A

Bosonisation dictionary

Here is a summary of important bosonisation formulae without proof. More detailed proofs about correlation functions can be found in [20, 23].

Fermionic field operator ψ and density operator ρ are given as

$$
\begin{aligned}
\psi(x) &= \psi_R(x) + \psi_L(x), \\
\rho(x) &= \psi^\dagger(x)\psi(x) = \rho_R(x) + \rho_L(x) + (\psi_R^\dagger(x)\psi_L(x) + \text{h.c.}).
\end{aligned}
\tag{A.1}
$$

In terms of bosonic field, the left/right moving fermionic field operators become

$$
\psi_r(x) = F_r \lim_{\alpha \to 0} \frac{1}{\sqrt{2\pi\alpha}} e^{ir(k_F - \pi/L)x} e^{-i(r\phi(x) - \theta(x))},
\tag{A.2}
$$

where F_r is the Klein factor, preserving the anticommutations between fermionic fields. In order to calculate of the correlation function, Klein factors can be treated as Majorana operators (i.e. real but anticommute with each other). For the bosonic fields $\phi(x)$ and $\theta(x)$, they are defined as

$$
\begin{aligned}
\phi(x) &= -(N_R + N_L)\frac{\pi x}{L} - \frac{i\pi}{L}\sum_{p\neq 0}\frac{1}{p}e^{-\alpha|p|/2 - ipx}[\rho_R^\dagger(p) + \rho_L^\dagger(p)], \\
\theta(x) &= (N_R - N_L)\frac{\pi x}{L} + \frac{i\pi}{L}\sum_{p\neq 0}\frac{1}{p}e^{-\alpha|p|/2 - ipx}[\rho_R^\dagger(p) - \rho_L^\dagger(p)],
\end{aligned}
\tag{A.3}
$$

with commutation relation

$$
[\phi(x), \frac{1}{\pi}\nabla\theta(x')] = i\delta(x' - x).
\tag{A.4}
$$

And the Hamiltonian becomes

$$
H = \frac{u}{2\pi}\left[K(\nabla\theta(x))^2 + \frac{1}{K}(\nabla\phi(x))^2\right],
\tag{A.5}
$$

A. BOSONISATION DICTIONARY

with renormalised Fermi velocity u, and Luttinger coefficient K related to the interaction.

Taking into account all the high harmonics in a general model, the field operators for hard-core boson ψ_B and fermion ψ_F and the density operator are

$$
\psi_B^\dagger(x) = \sqrt{\rho_0 - \frac{1}{\pi}\nabla\phi(x)} \sum_q e^{i2q(\pi\rho_0 x - \phi(x))} e^{-i\theta(x)},
$$

$$
\psi_F^\dagger(x) = F_r^\dagger \sqrt{\rho_0 - \frac{1}{\pi}\nabla\phi(x)} \sum_q e^{i(2q+1)(\pi\rho_0 x - \phi(x))} e^{-i\theta(x)}, \tag{A.6}
$$

$$
\rho(x) = \rho_0 - \frac{1}{\pi}\nabla\phi(x) + \rho_0 \sum_{q\neq 0} e^{i2q(\pi\rho_0 x - \phi(x))},
$$

with $q \in \mathbb{Z}$, ρ_0 being the average density.

One can also obtain the correlation functions with Hamiltonian A.5

$$
I = \langle \prod_j e^{i(A_j\phi(r_j) + B_j\theta(r_j))} \rangle, \tag{A.7}
$$

where $r_j = (x_j, \tau_j)$, A and B are coefficients that satisfy $\sum_j A_j = \sum_j B_j = 0$ to get non-vanishing correlation function I.

$$
I = \exp\left[-\frac{1}{2}\sum_{j<k}(-A_jA_kK - \frac{B_jB_k}{K})F_1(r_j - r_k) + (A_jB_k + B_jA_k)F_2(r_i - r_j) \right], \tag{A.8}
$$

with momentum cutoff $e^{-a|p|}, a \to 0$ and $T = 0$,

$$
F_1(r) = \frac{1}{2}\log\left[\frac{x^2 + (u|\tau| + a)^2}{a^2} \right],
$$
$$
F_2(r) = -i\mathrm{Arg}[y_a + ix], y_a = u\tau + a\mathrm{Sgn}(\tau). \tag{A.9}
$$

Acknowledgements

During my two-year master study in Stuttgart, I have met so many interesting people and there are many of them who I'm deeply indebted to. First of all, I would like to thank my supervisor Prof. Hans Peter B´uchler for accepting me to do the master thesis in the institute and helping me throughout the entire year of researching on many different aspects of physics. Without some deep and interesting discussions with you, I would never finish the thesis. Despite that my research direction is a bit different from now, I'm very grateful for all the knowledge and insights I've learnt from you.

In addition, I would like to thank my second supervisor, Prof. Maria Daghofer. Throughout the three courses of yours that I have participated, my passion for theoretical physics has been ignited, and you helped me with numerous discussions, some of which might be a bit trivial (from my current perspective).

Except for the mentors that I have in Stuttgart, I have enjoyed so much among my colleagues in ITP3. Most importantly, I would like to address my gratitude to Nicolai, Stephan and Daniel. Thank you Nicolai, for all the interesting discussions about topological phases of matter, CFT and your own research. Your broad knowledge of physics always encourages me to learn more. I can't wait to see more of your work in the future. Stephan, than you for being a great office mate, and sharing with me the broadness of strongly correlated systems. I don't know if you are going to choose China as your next destination, and if so, hope to see you there! Daniel, thank you for all the interesting discussions about spin systems (and lunch talks). Your advice helped me a lot while finding a PhD in Europe. All the best to your future job hunting! And of course many thanks to the rest of my

colleagues in ITP3, Jan, Sebastian, Tobi and Kevin, for all of your help and especially the volleyball tournament.

Beside the colleagues who helped me academically, I'm grateful for other physicists, who I met in workshops or had correspondences with. For the physicists who I met and had great discussions with, Mariana, Rubem, and Marcello, thank you guys for being interested in my research and giving some useful suggestions. Hope to see you guys again in some other workshops/conferences. Many thanks to Jean-Sébastien for sharing with me lots of interesting thoughts on Bethe ansatz and pointing out that alternating Heisenberg model can be solved via non-linear sigma model (and above all, accepting me as your PhD student). I'm grateful to Dr. Salvatore Manmana, Dr. Meng Cheng, Ruben Verresen, Prof. Benoît Grémaud, Prof. Erez Berg, and Prof. Gerardo Ortiz for their kind replies to my enquiries of their research and some further useful discussions and correspondences.

And of course many thanks to my classmates and other friends I've met in Stuttgart. My life would be much less interesting if you guys are not around. I wish you all to find the PhDs/jobs that you like, and can't wait to see you guys in Amsterdam or somewhere else in the earth. In addition, Mia, thank you for all of your help on the administrative stuff, without which I could not finish my master thesis.

The last but not the least, I would like to thank my parents and the whole family in China. Without your help throughout my life, I would never accomplish so much in my life. I wish good health and happiness to all of you.

References

[1] IMMANUEL BLOCH. **Ultracold quantum gases in optical lattices**. *Nature Physics*, **1**(1):23–30, 2005.

[2] IMMANUEL BLOCH, JEAN DALIBARD, AND WILHELM ZWERGER. **Many-body physics with ultracold gases**. *Reviews of modern physics*, **80**(3):885, 2008.

[3] SIMON BAIER, MANFRED J MARK, DANIEL PETTER, KIYOTAKA AIKAWA, LAURIANE CHOMAZ, ZI CAI, M BARANOV, P ZOLLER, AND F FERLAINO. **Extended Bose-Hubbard models with ultracold magnetic atoms**. *Science*, **352**(6282):201–205, 2016.

[4] CHRISTIAN TREFZGER, C MENOTTI, B CAPOGROSSO-SANSONE, AND M LEWENSTEIN. **Ultracold dipolar gases in optical lattices**. *Journal of Physics B: Atomic, Molecular and Optical Physics*, **44**(19):193001, 2011.

[5] EMANUELE G DALLA TORRE, EREZ BERG, AND EHUD ALTMAN. **Hidden order in 1D Bose insulators**. *Physical Review Letters*, **97**(26):260401, 2006.

[6] EREZ BERG, EMANUELE G DALLA TORRE, THIERRY GIAMARCHI, AND EHUD ALTMAN. **Rise and fall of hidden string order of lattice bosons**. *Physical Review B*, **77**(24):245119, 2008.

[7] FRANK POLLMANN, ARI M TURNER, EREZ BERG, AND MASAKI OSHIKAWA. **Entanglement spectrum of a topological phase in one dimension**. *Physical Review B*, **81**(6):064439, 2010.

[8] FRANK POLLMANN, EREZ BERG, ARI M TURNER, AND MASAKI OSHIKAWA. **Symmetry protection of topological phases in one-dimensional quantum spin systems**. *Physical Review B*, **85**(7):075125, 2012.

REFERENCES

[9] XIE CHEN, ZHENG-CHENG GU, AND XIAO-GANG WEN. **Classification of gapped symmetric phases in one-dimensional spin systems**. *Physical Review B*, **83**(3):035107, 2011.

[10] A YU KITAEV. **Unpaired Majorana fermions in quantum wires**. *Physics-Uspekhi*, **44**(10S):131, 2001.

[11] CHETAN NAYAK, STEVEN H SIMON, ADY STERN, MICHAEL FREEDMAN, AND SANKAR DAS SARMA. **Non-Abelian anyons and topological quantum computation**. *Reviews of Modern Physics*, **80**(3):1083, 2008.

[12] YUVAL OREG, GIL REFAEL, AND FELIX VON OPPEN. **Helical liquids and Majorana bound states in quantum wires**. *Physical Review Letters*, **105**(17):177002, 2010.

[13] JASON ALICEA. **New directions in the pursuit of Majorana fermions in solid state systems**. *Reports on Progress in Physics*, **75**(7):076501, 2012.

[14] DIETER JAKSCH, CHRISTOPH BRUDER, JUAN IGNACIO CIRAC, CRISPIN W GARDINER, AND PETER ZOLLER. **Cold bosonic atoms in optical lattices**. *Physical Review Letters*, **81**(15):3108, 1998.

[15] DIETER JAKSCH AND PETER ZOLLER. **The cold atom Hubbard toolbox**. *Annals of physics*, **315**(1):52–79, 2005.

[16] SEBASTIAN D HUBER, EHUD ALTMAN, HANS PETER BÜCHLER, AND GIANNI BLATTER. **Dynamical properties of ultracold bosons in an optical lattice**. *Physical Review B*, **75**(8):085106, 2007.

[17] F DUNCAN M HALDANE. **Nonlinear field theory of large-spin Heisenberg antiferromagnets: semiclassically quantized solitons of the one-dimensional easy-axis Néel state**. *Physical Review Letters*, **50**(15):1153, 1983.

[18] IAN AFFLECK, TOM KENNEDY, ELLIOTT H LIEB, AND HAL TASAKI. **Rigorous results on valence-bond ground states in antiferromagnets**. *Physical Review Letters*, **59**(7):799, 1987.

[19] Ian Affleck, Tom Kennedy, Elliott H. Lieb, and Hal Tasaki. **Valence bond ground states in isotropic quantum antiferromagnets**. *Communications in Mathematical Physics*, **115**(3):477–528, Sep 1988.

[20] Thierry Giamarchi. *Quantum physics in one dimension*. Oxford university press, 2004.

[21] Naoto Nagaosa. *Quantum field theory in strongly correlated electronic systems*. Springer Science & Business Media, 1999.

[22] Alexei M Tsvelik. *Quantum field theory in condensed matter physics*. Cambridge university press, 2007.

[23] Jan von Delft and Herbert Schoeller. **Bosonization for beginners— refermionization for experts**. *arXiv preprint cond-mat/9805275*, 1998.

[24] Jean-Sébastien Caux and Cristiane Morais Smith. **Celebrating Haldanes Luttinger liquid theory**. *Journal of Physics: Condensed Matter*, **29**(15):151001, 2017.

[25] Philippe Francesco, Pierre Mathieu, and David Sénéchal. *Conformal field theory*. Springer Science & Business Media, 2012.

[26] Alexander Seidel and Dung-Hai Lee. **The Luther-Emery liquid: Spin gap and anomalous flux period**. *Physical Review B*, **71**(4):045113, 2005.

[27] Steven R White. **Density matrix formulation for quantum renormalization groups**. *Physical Review Letters*, **69**(19):2863, 1992.

[28] Ulrich Schollwöck. **The density-matrix renormalization group in the age of matrix product states**. *Annals of Physics*, **326**(1):96–192, 2011.

[29] Frank Verstraete, Juan J Garcia-Ripoll, and Juan Ignacio Cirac. **Matrix product density operators: simulation of finite-temperature and dissipative systems**. *Physical Review Letters*, **93**(20):207204, 2004.

[30] Matthew B Hastings. **An area law for one-dimensional quantum systems**. *Journal of Statistical Mechanics: Theory and Experiment*, **2007**(08):P08024, 2007.

REFERENCES

[31] Jens Eisert, Marcus Cramer, and Martin B Plenio. **Colloquium: Area laws for the entanglement entropy**. *Reviews of Modern Physics*, **82**(1):277, 2010.

[32] Norbert Schuch. **Condensed matter applications of entanglement theory**. *arXiv preprint arXiv:1306.5551*, 2013.

[33] CM Herdman, P-N Roy, RG Melko, and Adrian Del Maestro. **Entanglement area law in superfluid ^{4}He**. *Nature Physics*, **13**(6):556–558, 2017.

[34] Pasquale Calabrese and John Cardy. **Entanglement entropy and quantum field theory**. *Journal of Statistical Mechanics: Theory and Experiment*, **2004**(06):P06002, 2004.

[35] Pasquale Calabrese and John Cardy. **Entanglement entropy and conformal field theory**. *Journal of Physics A: Mathematical and Theoretical*, **42**(50):504005, 2009.

[36] Maria Hermanns. **Entanglement in topological systems**. *arXiv preprint arXiv:1702.01525*, 2017.

[37] Alexei Kitaev and John Preskill. **Topological entanglement entropy**. *Physical Review Letters*, **96**(11):110404, 2006.

[38] Michael Levin and Xiao-Gang Wen. **Detecting topological order in a ground state wave function**. *Physical Review Letters*, **96**(11):110405, 2006.

[39] Hui Li and F Duncan M Haldane. **Entanglement spectrum as a generalization of entanglement entropy: Identification of topological order in non-abelian fractional quantum hall effect states**. *Physical Review Letters*, **101**(1):010504, 2008.

[40] Benoît Grémaud and G George Batrouni. **Haldane phase on the sawtooth lattice: Edge states, entanglement spectrum, and the flat band**. *Physical Review B*, **95**(16):165131, 2017.

[41] David Pérez-García, Michael M Wolf, M Sanz, Frank Verstraete, and J Ignacio Cirac. **String order and symmetries in quantum spin lattices**. *Physical review letters*, **100**(16):167202, 2008.

[42] Xie Chen, Zheng-Cheng Gu, and Xiao-Gang Wen. **Local unitary transformation, long-range quantum entanglement, wave function renormalization, and topological order**. *Physical Review B*, **82**(15):155138, 2010.

[43] Xie Chen, Zheng-Cheng Gu, Zheng-Xin Liu, and Xiao-Gang Wen. **Symmetry-protected topological orders in interacting bosonic systems**. *Science*, **338**(6114):1604–1606, 2012.

[44] Tom Kennedy and Hal Tasaki. **Hidden $\mathbb{Z}_2 \times \mathbb{Z}_2$ symmetry breaking in Haldane-gap antiferromagnets**. *Physical Review B*, **45**(1):304, 1992.

[45] Tom Kennedy and Hal Tasaki. **Hidden symmetry breaking and the Haldane phase in S= 1 quantum spin chains**. *Communications in mathematical physics*, **147**(3):431–484, 1992.

[46] Masaki Oshikawa. **Hidden $\mathbb{Z}_2 \times \mathbb{Z}_2$ symmetry in quantum spin chains with arbitrary integer spin**. *Journal of Physics: Condensed Matter*, **4**(36):7469, 1992.

[47] Dominic V Else, Stephen D Bartlett, and Andrew C Doherty. **Hidden symmetry-breaking picture of symmetry-protected topological order**. *Physical Review B*, **88**(8):085114, 2013.

[48] Kouichi Okunishi. **Topological disentangler for the valence-bond-solid chain**. *Physical Review B*, **83**(10):104411, 2011.

[49] Jason Alicea and Paul Fendley. **Topological phases with parafermions: theory and blueprints**. *Annual Review of Condensed Matter Physics*, **7**:119–139, 2016.

[50] Lukasz Fidkowski and Alexei Kitaev. **Topological phases of fermions in one dimension**. *Physical Review b*, **83**(7):075103, 2011.

[51] Paul Fendley. **Parafermionic edge zero modes in $\mathbb{Z}_N$-invariant spin chains**. *Journal of Statistical Mechanics: Theory and Experiment*, **2012**(11):P11020, 2012.

[52] Paul Fendley. **Free parafermions**. *Journal of Physics A: Mathematical and Theoretical*, **47**(7):075001, 2014.

REFERENCES

[53] ADAM S JERMYN, ROGER SK MONG, JASON ALICEA, AND PAUL FEND-LEY. **Stability of zero modes in parafermion chains**. *Physical Review B*, **90**(16):165106, 2014.

[54] PAUL FENDLEY. **Strong zero modes and eigenstate phase transitions in the XYZ/interacting Majorana chain**. *J. Phys. A: Math. Theor.*, **49**:30LT01, 2016.

[55] EMILIO COBANERA, GERARDO ORTIZ, AND ZOHAR NUSSINOV. **The bond-algebraic approach to dualities**. *Advances in Physics*, **60**(5):679–798, 2011.

[56] FRANK VERSTRAETE, J IGNACIO CIRAC, JI LATORRE, E RICO, AND MICHAEL M WOLF. **Renormalization-group transformations on quantum states**. *Physical Review Letters*, **94**(14):140601, 2005.

[57] RUBEN VERRESEN, RODERICH MOESSNER, AND FRANK POLLMANN. **One-Dimensional Symmetry Protected Topological Phases and their Transitions**. *arXiv preprint arXiv:1707.05787*, 2017.

[58] F DUNCAN M HALDANE. **Continuum dynamics of the 1-D Heisenberg antiferromagnet: identification with the O (3) nonlinear sigma model**. *Physics Letters A*, **93**(9):464–468, 1983.

[59] IAN K AFFLECK. **Field theory methods and quantum critical phenomena**. Technical report, PRE-31353, 1988.

[60] DAVID PETER, STEFFEN MÜLLER, STEFAN WESSEL, AND HANS PETER BÜCHLER. **Anomalous behavior of spin systems with dipolar interactions**. *Physical Review Letters*, **109**(2):025303, 2012.

[61] Z-X GONG, MOHAMMAD F MAGHREBI, ANZI HU, MICHAEL L WALL, MICHAEL FOSS-FEIG, AND ALEXEY V GORSHKOV. **Topological phases with long-range interactions**. *Physical Review B*, **93**(4):041102, 2016.

[62] Z-X GONG, MOHAMMAD F MAGHREBI, ANZI HU, MICHAEL FOSS-FEIG, PHILLIP RICHERME, CHRISTOPHER MONROE, AND ALEXEY V GORSHKOV. **Kaleidoscope of quantum phases in a long-range interacting spin-1 chain**. *Physical Review B*, **93**(20):205115, 2016.

[63] Salvatore R Manmana, Marcel Möller, Riccardo Gezzi, and Kaden RA Hazzard. **Correlations and enlarged superconducting phase of $t - J_\perp$ chains of ultracold molecules on optical lattices**. *arXiv preprint arXiv:1707.00343*, 2017.

[64] Xiaolong Deng and Luis Santos. **Entanglement spectrum of one-dimensional extended Bose-Hubbard models**. *Physical Review B*, **84**(8):085138, 2011.

[65] Waseem S Bakr, Jonathon I Gillen, Amy Peng, Simon Fölling, and Markus Greiner. **A quantum gas microscope-detecting single atoms in a Hubbard regime optical lattice**. *Nature*, **462**:74–77, 2009.

[66] Ahmed Omran, Martin Boll, Timon A Hilker, Katharina Kleinlein, Guillaume Salomon, Immanuel Bloch, and Christian Gross. **Microscopic observation of Pauli blocking in degenerate fermionic lattice gases**. *Physical review letters*, **115**(26):263001, 2015.

[67] Timon A Hilker, Guillaume Salomon, Fabian Grusdt, Ahmed Omran, Martin Boll, Eugene Demler, Immanuel Bloch, and Christian Gross. **Revealing hidden antiferromagnetic correlations in doped Hubbard chains via string correlators**. *arXiv preprint arXiv:1702.00642*, 2017.